

SYNTHESIS AND CRYSTAL CHEMISTRY OF $\text{Ca}_2\text{N}_x\text{O}_{2-2x}\text{F}_x$ ($x = 0$ to 1) AND
OTHER COMPOUNDS

By

Michael S. Strozewski

Submitted in Partial Fulfillment of the Requirements

for the Degree of

Master of Science

in the

Chemistry

Program

Youngstown State University

August, 2007

SYNTHESIS AND CRYSTAL CHEMISTRY OF $\text{Ca}_2\text{N}_x\text{O}_{2-2x}\text{F}_x$ ($x = 0$ to 1) AND
OTHER COMPOUNDS

Michael S. Strozewski

I hereby release this thesis to the public. I understand this thesis will be housed at the Circulation Desk of the University Library and will be available for public access. I also authorize the University or other individuals to make copies of this thesis as needed for scholarly research.

Signature:

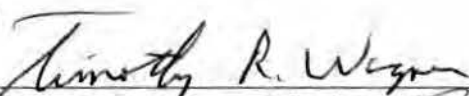


Michael S. Strozewski, Student

8-10-07

Date

Approvals:



Dr. Timothy R. Wagner, Thesis Advisor

8/13/07

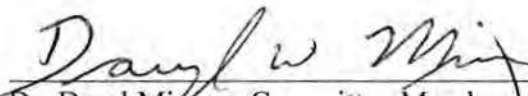
Date



Dr. Allen D. Hunter, Committee Member

8/13/07

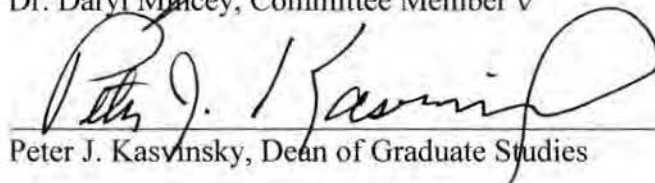
Date



Dr. Daryl Mincey, Committee Member

8/17/07

Date



Peter J. Kasvinsky, Dean of Graduate Studies

8/16/07

Date

ABSTRACT

Study of the $\text{Ca}_2\text{N}_x\text{O}_{2-2x}\text{F}_x$ system through single-crystal X-ray diffraction experiments was done to test the air stability of these compounds, and to subsequently synthesize a “pure” Ca_2NF sample. Several syntheses were done to purposefully introduce oxygen into the lattice and to eliminate it from the lattice. Results show a range of oxygen content over a number of characterized structures in this system. The Imma phase of $\text{Ca}_2\text{Fe}_2\text{O}_5$ was characterized at room temperature for the first time with synchrotron data from the Advanced Light Source at Berkeley Labs, CA and additional X-ray microanalysis data provided by the Materials Research Laboratory in Struthers, OH.

ACKNOWLEDGMENTS

I would like to thank everyone in the YSU chemistry department for all the guidance and helpfulness you have shown me while being a student at YSU. I am not a teacher but all the knowledge I have attained at YSU and abroad is a direct result of the interactions with great teachers of chemistry and I hope that I can one day be as good a teacher, in chemistry or in whatever I am doing, as the teachers I have had the pleasure of meeting throughout my education. I have to thank Dr. Wagner the most for helping me achieve this degree because he has been the best advisor a person could ever ask for. He is always there to answer your questions and give you advice on any subject. I learned so much from him, in and out of the classroom, and feel more enlightened as a person as a result. I would also like to thank my other committee members, Dr. Hunter and Dr. Mincey, for critiquing my work. Thanks also to Kris Gregory for getting me out of numerous pickles as it pertains to paperwork and things of that nature.

I also must thank my parents for giving me the opportunity and encouraging me to further my education. I know I don't say it enough, but I love you both more than words can express. I want to thank Dr. David Moss, Dr. John Cragel and Dr. John Andrews of Hiram College. My numerous classes with these three professors inspired me to want to learn more about chemistry and to further my education in this wonderful subject. I am happy not to just call them former professors, but to be able to call them friends. Finally, I have to thank my best

friend Carol. I can't wait to spend the rest of my life with you and promise to love you with all my heart each and every day we have together on this Earth.

To anyone I didn't mention personally, I don't have enough room to acknowledge everyone, otherwise this section would be longer than my entire thesis.

TABLE OF CONTENTS

	PAGE
TITLE PAGE.....	i
SIGNATURE PAGE.....	ii
ABSTRACT.....	iii
ACKNOWLEDGMENTS.....	iv
TABLE OF CONTENTS.....	v
LIST OF TABLES.....	vii
LIST OF FIGURES.....	viii
CHAPTERS.....	
I. SOLID STATE CHEMISTRY.....	1
Introduction.....	1
Solid State Synthesis.....	2
Types of Crystalline Solids.....	5
Bonding in Solids.....	7
X-ray Diffraction.....	9
Synchrotron Diffraction.....	14
The Single-Crystal X-ray Diffraction Experiment.....	16
Bond Valence Sum Theory.....	19
II. PEROVSKITES AND NITRIDE FLUORIDES.....	21
Perovskite Background.....	21
Nitride Fluoride Background.....	25
III. STATEMENT OF THE PROBLEM.....	31

IV.	METHODS AND MATERIALS.....	33
	Crystal Mounting.....	33
	Single-Crystal Data Collection and Analysis.....	34
V.	EXPERIMENTAL RESULTS.....	35
	Preparation of $\text{Ca}_2\text{N}_x\text{O}_{2-2x}\text{F}_x$ Compounds.....	35
	Proposed Synthesis of CaMnNF_2	40
	Attempted Synthesis of SrMnNF_2	43
	Attempted Synthesis of BaMnNF_2	44
VI.	DISCUSSION.....	47
	$\text{Ca}_2\text{N}_x\text{O}_{2-2x}\text{F}_x$ System.....	47
	$\text{Ca}_2\text{Fe}_2\text{O}_5$ System.....	50
	REFERENCES.....	61
	APPENDIX A.....	64
	APPENDIX B.....	73

LIST OF TABLES

TABLE	PAGE
2.1 Summary of Some Perovskite Compounds and Their Tolerance Factors.....	24
2.2 Summary of Known M_2NF Compounds.....	28
6.1 Compositional Estimates of $Ca_2N_xO_{2-2x}F_x$ Phases.....	49
6.2 Comparison of $Ca_2Fe_2O_5$ Structural Data for Literature vs. This Study.....	55
A-1 Crystal data and structure refinement for $Ca_2Mn_2N_2O_2F$	65
A-2 Atomic coordinates ($\times 10^4$) and equivalent isotropic displacement parameters ($A^2 \times 10^3$) for $Ca_2Mn_2N_2O_2F$	66
A-3 Bond lengths [A] and angles [deg] for $Ca_2Mn_2N_2O_2F$	67
A-4 Anisotropic displacement parameters ($A^2 \times 10^3$) for $Ca_2Mn_2N_2O_2F$	72
B-1 Crystal data and structure refinement for $Ca_2Fe_2O_5$	74
B-2 Atomic coordinates ($\times 10^4$) and equivalent isotropic displacement parameters ($A^2 \times 10^3$) for $Ca_2Fe_2O_5$	75
B-3 Bond lengths [A] and angles [deg] for $Ca_2Fe_2O_5$	76

LIST OF FIGURES

FIGURE	PAGE
1.1 Example of Face-Centered-Cubic Structures.....	6
1.2 X-ray Diffraction Setup.....	11
1.3 Diffraction of X-rays from crystalline planes.....	12
1.4 Layout of How Synchrotron Diffraction Works and What the Advanced Light Source at Berkeley Looks Like.....	15
2.1 A Perovskite Structure.....	22
2.2 Three different reported structure types of compounds of M_2NF formula.....	29
6.1 Ball and Stick Refinement of $Ca_2Fe_2O_5$	53
6.2 Fe(2) and O(3) 50% Occupied Environment.....	54
6.3 Comparison of Reported Literature Phase and Our Experimental Phase.....	57
6.4 Right and Left Handed Chains of FeO_4	58
6.5 Orientation of the Fe(2) Chains in the Unit Cell.....	59

CHAPTER I

SOLID STATE CHEMISTRY

Introduction

The field of solid state chemistry plays a very important role in the production of novel electrical and mechanical devices. Though molecular substances make up the majority of known compounds, it is important to understand the chemical and physical properties of solid state materials if the solid state chemist is going to continue to make advances in this field. Solid state chemists focus on developing new materials, not only for the hope of discovering new phenomena or enhanced properties, but also to understand the complexities of the many different bonding arrangements of the elements of the periodic table.¹ However, there are many challenges in the field of solid state chemistry that prevent the development of a sort of blueprint for the production of new materials like there is for organic molecules. There is a set of rules, named the "rational synthetic method" that guides the synthesis and invention of new organic compounds. Unfortunately, this set of rules is not applicable on extended solids and no such set of rules is known for non-molecular solids. Thus, solid state chemistry is an area that has a wealth of possibilities for the advancement of a more systematic synthetic approach to developing new compounds. Minor advances have been made in the study of binary compounds of generic formulas with small whole numbers (MX , MX_2 , MX_3 , M_3X_5 , etc.) and about 5% of the

100,000 possible ternary compounds. Unfortunately, beyond the binary compounds, prediction of the stoichiometric relationship within predicted compounds is not very good. In addition, not much exploration has been done with quaternary or quinary compounds, mainly because there are so many possibilities for these types of structures and there may be a preference of 5 element systems to form mixtures of binary and ternary compounds. Despite the advances from the studies of simpler compounds, there are still many factors of a solid state reaction that are unpredictable, such as nucleation, initial diffusion, diffraction and the overall kinetics of the reaction.

Solid State Synthesis

The best place to start understanding solid state materials is with the synthesis of these types of materials and everything that must be considered before synthesis even begins. There are many important properties that one must consider before selecting a synthetic method, but some of the more significant ones include diffusion rate or mass within and between solid particles. Thus, successful solid state reactions are dependent on these slow and highly variable processes for the production of homogeneous and single-phase products. As a result, high temperatures are generally used to improve the rates of synthesis of solid state materials.

There are many methods for preparing solid state materials but the most common is the exchange reaction because it can involve solids, liquids and gases to create a desired product of either of these phases. The generic blueprint for

these types of reactions is as follows: $A(l,s) + B(l,s) \rightarrow D(s)$. Liquids are much better than solids because they provide better contact and mobility for reaction to form product D, and so when using a molecular melt, there is much better mixing among these reactants. In order to successfully run this type of reaction with a molecular melt and avoid diffusion limitations, it is best to run the reaction above the melting temperature of the reactants². However, running the reaction below the melting temperature of the target product will often yield a finely divided and amorphous solid. More often than not, solid state reactions are repeated under different temperature conditions before the desired target compound is prepared.

Without question, solid state synthesis of air-sensitive products is a very tedious process because of the obvious need to keep air out of the reaction chamber. It is necessary to take every possible precaution to ensure purity when the products are being made for specific property applications, including the use of an inert atmosphere via a glove bag or glove box, high purity gases, or good high vacuum. It is also important to take care of your products and increase their purity through techniques such as recrystallization, ignition, drying, sublimation and transport of starting materials before and after preparation. Purities over 99% are the minimum to consider a compound pure. Many solid state materials are polycrystalline in which case X-ray powder diffraction is the best place to start to determine purity. The Debye-Scherrer method for powder analysis used to be the likely method to start with, but formation of separate phases of crystalline materials during synthesis are very possible and the Debye-Scherrer method can miss up to 10% or more of another phase and provide poor resolution. In addition,

the method is outdated and not nearly as effective as the newer, more technologically advanced methods. Therefore, the X-ray diffractometer should be used. With this technique, it is easier to recognize substitution impurities and the effects of non-stoichiometry because lattice dimensions obtained from least-squares analysis and high angle refinement data are compared. This method regularly obtains standard deviations around .01%. Other techniques include optical microscopy, microprobe, and X-ray fluorescence, but X-ray diffraction will be the method of choice for this project, since the major goal is to describe the structures of newly prepared materials and relate them to properties where appropriate.

When deciding how to design a successful solid state reaction, it is important to consider such factors as thermodynamics and kinetics of the reactants, as well as phase relationships and the employment of high temperatures and pressures. Of course, a lot of these factors depend on the availability of pure and inexpensive reactants and the presence of certain mechanistic problems like material transport. These mechanistic problems are the reason that many solid state reactions employ gaseous and liquid reactants and solvents. These factors have influenced the synthetic procedures that will be described later in this thesis and have proven to be quite successful in the production of single crystalline products.

Types of Crystalline Solids

Solid state materials are classified into the following categories: metals and alloys, ionic structures, covalent network structures, and molecular structures. Metals generally crystallize into one of three arrangements: hexagonal close packed (h.c.p.), cubic close packed (c.c.p.) and body centered cubic (b.c.c.). Metals don't follow any predictable trends as to which of these arrangements they fall into, and the reason for this is not well understood². Alloys are intermetallic phases and are like pure metals in that many of them are regarded as close packed structures. There is a wide range of ionic structures that can be grouped into six main classes that share the characteristics of being c.c.p or h.c.p., some of which are depicted in Figure 1.1. In many ionic structures, the anion is larger than the cation and these structures can be characterized as close packed layers of anions with cations placed in interstitial sites. When the cations are too big, the structure can only accommodate them by expanding the anion array and as a result, the arrangement of the anions is the same as in a close packed structure but the ions aren't necessarily touching. Ionic structures can first be characterized as having, for example, the rocksalt or nickel arsenide structure, where they both have octahedrally coordinated cations and only differ in their anion stacking sequence². Compounds with the rocksalt structure are c.c.p., and compounds with the nickel arsenide are h.c.p. Some other ionic structures include zinc blende (ZnS), rutile (TiO₂), antiferite (K₂O), spinel (MgAl₂O₄) and perovskite (CaTiO₃). The compounds discussed later in this thesis will be of the rocksalt-type and perovskite-type structures. The final two types of crystalline solids, covalent

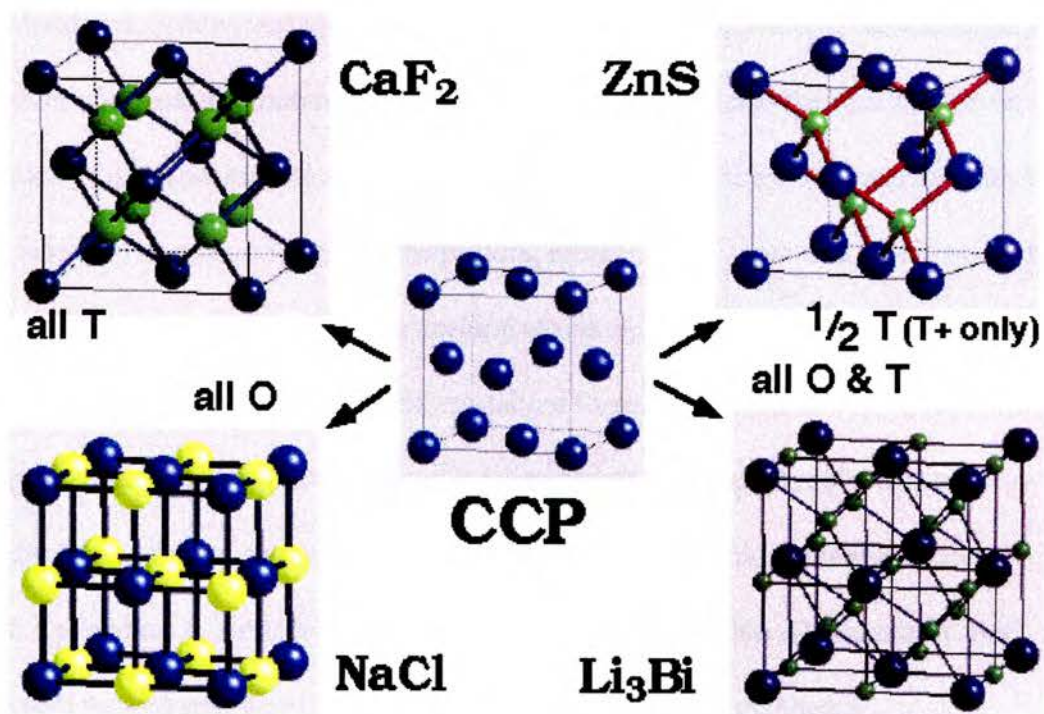


Figure. 1.1 Example of Face-Centered-Cubic Structures²⁵

network structures and molecular structures, were not a major part of the research for this thesis, but basic knowledge of these structures is important. Diamond and silicon carbide are examples of covalent network solids and can be described as close packed or eutactic structures and many network solids are similar to ionic structures. Silicon carbide can be classified as having the wurtzite structure and a three-dimensional framework of corner sharing tetrahedra is the result if silicon or carbon is the packing atom. Diamond has the sphalerite ionic structure and can be described as eutactic since all the packing atoms are the same size and it would be hard to distinguish between the packing atoms and the interstitial atoms.

Molecular structures, such as the crystalline forms of H_2 , CH_4 and HCl , form close packed structures even though the bonding forces of adjacent molecules are van der Waal's forces. Spherical molecules like the ones mentioned above fit into h.c.p. and c.c.p. structures, but non-spherical molecules like Al_2Br_6 can fit into close packed structures if they are built of tetrahedra and octahedra².

Bonding in Solids

Crystalline solids display many types of bonding, from ionic, covalent, metallic and van der Waal's. However, very often crystalline solids will have a mixture of these common bond types. For example, TiO has a mixture of ionic and metallic bonding and CdI_2 has a mixture of ionic, covalent and van der Waal's bond types. Crystal structures with ionic bonding tend to have high symmetry and coordination numbers that are as high as possible. Thus, the lattice energy of the crystal is maximized because the net electrostatic attractive force is also

maximized. On the contrary, covalently bonded solids have low coordination numbers because many of the atoms present have a preference for a certain coordination environment and highly directional bonds are the result. Interestingly enough, covalent solids with atoms of similar size of a corresponding ionic structure may have lower coordination numbers, despite the size similarities. Although most ionic structures are looked at as purely ionic in character, this assumption is almost impossible in practice. Even structures like NaCl, which is usually regarded as a pure ionic solid, has some degree of covalent bonding in it. Observations of this increasing covalent character in ionic solids have been made and some explanations have been proposed. For example, when you look at SrO, BaO and HgO in terms of radius ratios, you would expect HgO to have the octahedrally coordinated rocksalt structure like BaO and SrO. However, mercury has a coordination of two in the HgO structure and this can be rationalized with *sp* hybridization theory. Hybridization of the 6*s* and 6*p* orbitals of the first excited state of mercury gives rise to two linear *sp* hybrids. Each of these hybrid orbitals forms a normal covalent bond by overlap with an oxygen orbital and therefore, mercury has a coordination of two. Another observation of the integration of covalent character to essentially ionic structure is with the following group of compounds: AlF₃, AlCl₃, AlBr₃ and AlI₃. As you move down this group, you go from AlF₃, which is essentially ionic in nature, to AlBr₃ and AlI₃ which are basically covalent molecules. The apparent explanation for this effect is the fact that the electronegativity difference is decreasing as you go down the group and the covalent character is increasing.

X-ray Diffraction

Crystallography has been helping chemists learn more about crystals and their properties for hundreds of years. Looking at the symmetry, lattice points, geometries, space groups and many of the other aspects of crystals, one can gain a basic vocabulary for understanding crystallography. Single crystal X-ray diffraction, combined with crystallographic analysis, is widely recognized as the best available technique for determining structures of unknown crystalline materials, whether they are molecular or non-molecular in character. X-rays are on the electromagnetic spectrum between gamma rays and ultraviolet rays and the X-rays used in diffraction experiments are produced when a beam of electrons collides with a metal target, usually copper, after being accelerated through 30-50 KV. The accelerated electrons originate from a heated tungsten filament and collide with a copper or other metal target. The X-rays are produced as a result of the high-energy electrons ionizing some of the 1s electrons of copper. A 2p or 3p electron immediately drops down to occupy the 1s level and the result is X-radiation with fixed transition energies and a spectrum of characteristic X-rays. The transition of copper's 2p→1s is called $K\alpha$ and the transition of the 3p→1s is called $K\beta$. There are actually two $K\alpha$'s, named $K\alpha_1$ and $K\alpha_2$, and the weaker $K\alpha_2$ can be removed if so desired, otherwise one may see a doublet from the $K\alpha$ with wavelengths 1.54051 Å for $K\alpha_1$ and 1.54433 Å for $K\alpha_2$. $K\beta$ has a wavelength of 1.3922 Å, but the $K\alpha_1$ radiation is more intense and occurs more frequently and so the $K\alpha$ is the radiation that is used in most diffraction experiments. The beam escapes the X-ray tube through beryllium windows because beryllium is of low

atomic weight and won't significantly absorb the radiation produced inside the tube. The beam then passes through a graphite or other monochromator that removes the $K\beta$, and possibly the $K\alpha_2$, as well as a broad spectrum of wavelengths known as "white radiation". A typical X-ray diffraction setup can be seen in Figure 1.2.

One of the first proposed mathematical explanations for the diffraction of X-rays was by Laue. The Laue equation is derived by looking at a crystal as an array of one-dimensional lines of atoms, and treating diffraction of X-rays from such a crystal just like diffraction of light from an optical grating. The equation relates the separation of the atoms, a , the X-ray wavelength, λ , and the diffraction angle, ϕ to give the equation: $a \sin\phi = n\lambda$. Of course, real crystals are three-dimensional and so three Laue equations are required, one for each of the axes representing the atomic arrangement of the crystal, and these must be solved simultaneously for diffraction to be modeled successfully. This method is mathematically correct but it is very hard to manage and this property led to the almost universal usage of Bragg's Law to decipher diffraction by crystals. Bragg's Law uses an approach to crystals that regards them as layers of semi-transparent mirror planes with X-rays bombarding the planes. As depicted in Fig. 1.3, some of the X-rays are reflected off the first plane and the subsequent planes reflect ones that are not reflected by the first plane. It is important to mention and understand that the incident angle of the X-rays is equal to the angle of reflection of the

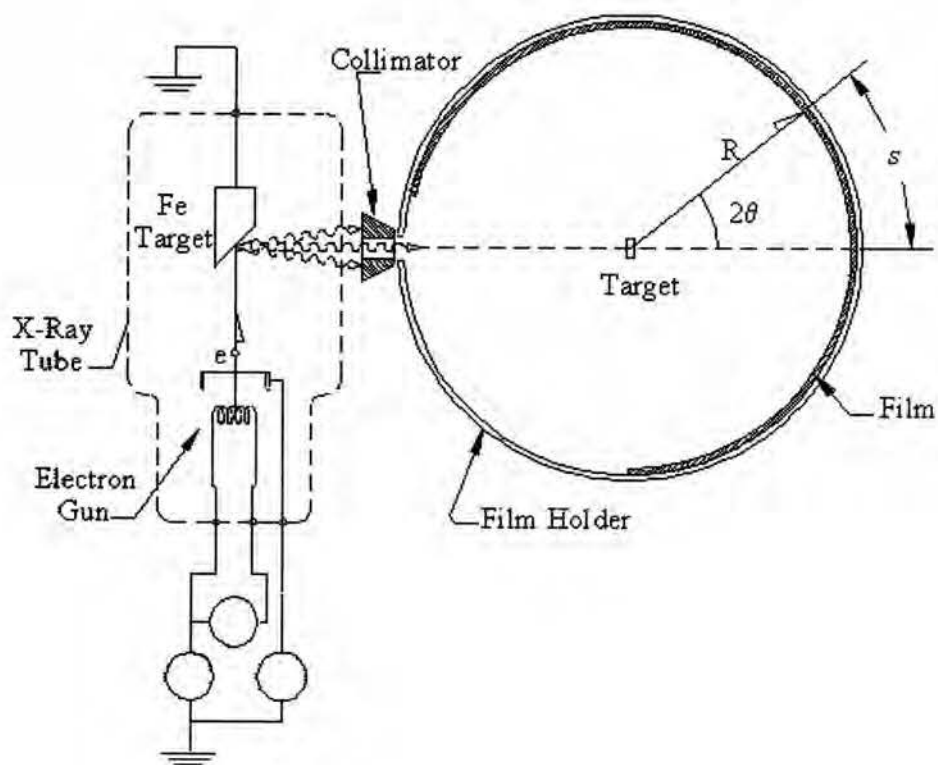


Figure 1.2 X-ray Diffraction Setup²⁶.

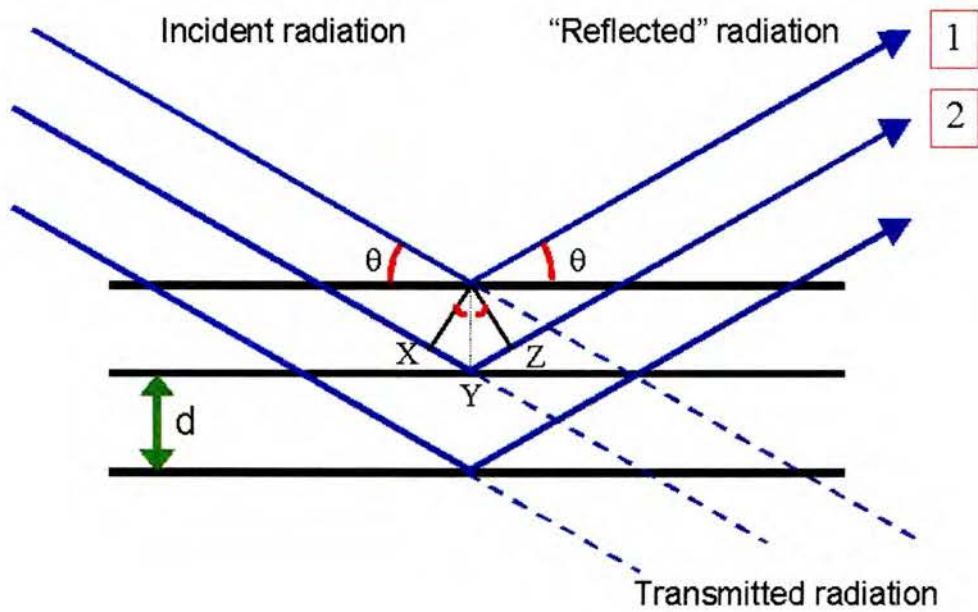


Fig. 1.3: Diffraction of X-rays from crystalline planes²⁷

X-rays. The reflected X-rays are in phase and interfere constructively when Bragg's Law is obeyed, but when the incident angle is anything but the Bragg angle, the reflected rays interfere destructively because they are out of phase.

Bragg's Law is given by the formula: $2d \sin\theta = n\lambda$, where d is the perpendicular distance between pairs of adjacent planes, or the d -spacing, and θ is the angle of incidence or *Bragg angle*. For a given set of these theoretical mirror planes, there are several solutions of the Bragg equation where n , on the order of reflections, is any integer. Usually, n is set to 1 and higher order reflections are treated as originating from smaller d -spacings. For example, when n is 2, the d -spacing is cut in half and this keeps n at 1 by doubling the number of planes in the set. In reality, a higher order reflection can occur whenever θ is large enough that there are wavelengths of difference in path lengths between successive planes. Bragg diffraction is the basis for the concept of Miller indices and Miller planes.

Despite the usefulness of Bragg's Law, it has three limitations that should be mentioned. The first one is that Bragg's Law says nothing about the intensities of the diffracted X-rays. Intensities are important because they are absolutely necessary for determining unknown crystal structures because the intensities given by a specific crystal act as a sort of fingerprint for that crystal structure. Second, Bragg's Law says nothing about the systematic absences that occur in many crystal structures. The atomic planes that are used as the backbone to Bragg's Law can sometimes give rise to these systematic absences where the intensity of the diffracted beam is zero. These systematic absences arise when the lattice type is non-primitive or if symmetry elements like screw axes and glide planes are

present. Therefore, systematic absences are very important in deducing the inherent symmetry present in a crystal. The last limitation of Bragg's Law is that it does not say anything about the physics of the diffraction. Bragg's Law says nothing about the physical interactions between the electron clouds of the atoms in the crystal and the incident X-rays, among other things.

Synchrotron Diffraction

The synchrotron diffraction data in this thesis comes from the Advanced Light Source (ALS) at Berkeley Labs in California, a research facility that analyzes crystalline structures to resolution of less than 0.70 \AA . A schematic of the layout of the ALS facility is shown in Figure 1.4. The main advantage of the ALS facility is that it produces X-rays that are brighter than any other X-ray source in America and these X-rays have wavelengths the size of atoms and molecules. As a result, these X-rays have suitable energies to interact with light atoms like carbon and oxygen. Normal X-ray tubes do not produce bright enough X-rays for high-resolution experiments because acceleration energies used to produce the beam are relatively small. High resolution experiments are possible with lab diffractometers, the problem is the intensity of the data. The analogy to use for comparing normal X-ray tubes and ALS is that normal X-rays are like a flood light and ALS X-rays are like a laser and they have other advantages besides their brightness, like tunability, near-coherence, pulsed nature and polarization. The Advanced Light Source is much larger than regular X-ray devices because its largest component, the storage ring, is roughly two-thirds the size of a

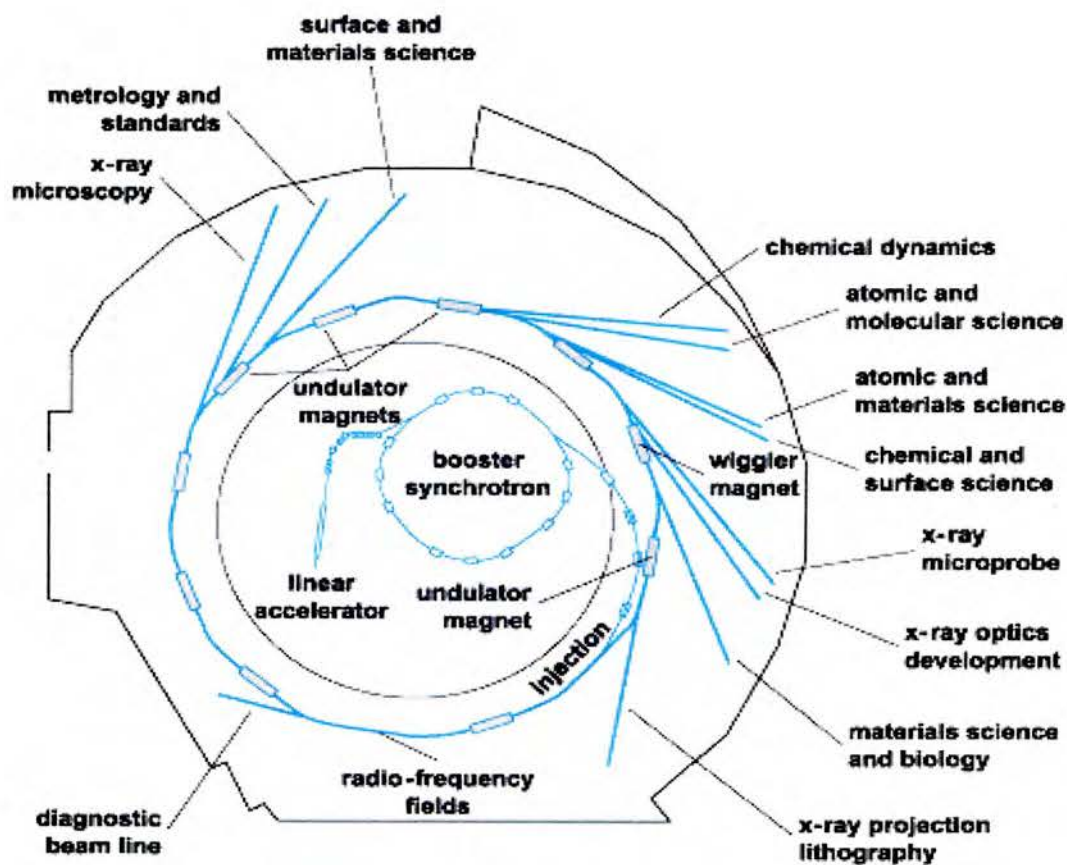


Figure 1.4 Layout of How Synchrotron Diffraction Works and What the Advanced Light Source at Berkeley Looks Like²⁸.

football field. The storage ring is a tubular vacuum chamber and it is so big because it has to hold an electron beam traveling at nearly the speed of light and maintain its energy³⁰. The electrons give off light as they circle the ring and the ring maintains the energy of the electron beam at 1.5-1.9 billion electron-volts, the energy required to produce light of the wavelength and brightness needed to explore properties of materials that a regular X-ray machine cannot do.

The Single-Crystal X-ray Diffraction Experiment

In order to dissect an unknown crystal and identify its structure, it is important to understand the technique that is commonly used by chemists, X-ray diffraction (XRD). There are two main X-ray methods used to determine unknown structures and they are the X-ray powder diffraction and single-crystal X-ray diffraction. The advantage of X-ray powder diffraction over single-crystal X-ray diffraction is that it is easier to prepare a powder sample and you are guaranteed to see all the reflections of the crystal system, unlike the case for serial detector single-crystal systems. However, determining the structure based on the measured intensities of the X-ray reflections is much harder and far less reliable than single-crystal X-ray diffraction. Therefore, single-crystal X-ray diffraction is the preferred choice for structure determination in general and throughout this thesis and the discussion given here will focus on that technique. The main disadvantage of single-crystal X-ray diffraction is the relative difficulty in preparing single crystalline samples because even if you have a single crystal, it may not be truly single crystalline. Thusly, if more than one phase is present it

may not be possible to determine the structure, although this is becoming less of a problem with the advances in crystallographic software.

Preparing the crystalline samples required for single-crystal X-ray diffraction is difficult, as the crystals in our project tend to be very small and they must be mounted inside tiny capillaries to be protected from air as X-rays bombard them. It is important to choose a crystal of appropriate size because for anything larger than the X-ray beam itself, absorption becomes a problem. On the contrary, anything too small will not diffract sufficiently to give enough data of necessary high intensity.

Mounting the small crystals obtained for this study is very tedious work. Everything is so small and fragile that you must have excellent hand-eye coordination to implement this technique, which will be described more fully later on. Once the sample is mounted and centered properly so that the most intense portion of the X-ray beam hits the crystal from every direction, the crystal can usually be characterized from the resulting data that is collected. Solving an unknown structure is dependent on the amount and quality of high intensity data that is obtained, because these intensities depend entirely on the identities and relative positions of the atoms present. Therefore, you need a large amount of high intensity data in order to refine this data to an optimal structure and, in general, most research journals require a data/parameter ratio of about 8 to 1 for publication quality work. The main reason for the need for a large data/parameter ratio is that it is required for the structure solution method employed by the crystallographic software. As an example, TiO_2 requires only three variables, or

parameters, to describe its structure, meaning that only about 20 independent reflections would be necessary to determine the structure by single-crystal X-ray diffraction, and it likely could be just as readily determined with powder diffraction. A more complex compound like $\text{YBa}_2\text{Cu}_3\text{O}$ gives 14 variables and requires 200-300 independent intensities for a good structure determination, and this would have to be solved with single-crystal X-ray diffraction or high-resolution neutron diffraction because routine powder methods do not give enough well resolved reflections. More complicated structures like silicates and complex organic molecules require 2,000-3,000 intensities because these types of molecules routinely have 50-100 variables. In general, the lower the symmetry of the crystal, the larger the number of variables that must be determined in order to solve the structure.

In order to solve the structure after data collection, the intensity data is corrected for polarization factors and other effects and converted to observed structure factors, F^{obs} . This process, however, leads to the inevitable phase problem of structure determination. The intensity data and observed structure factors undergo a Fourier transform to provide an electron density map where the atomic coordinates can be determined as the corrected structure factors are obtained using the formula $F^{\text{obs}} = \sqrt{I^{\text{obs}}}$. As a result, the phase of F^{obs} is not directly obtained while the amplitude is. This is because the \sqrt{I} values must be positive but the F values may be positive or negative, and thus, we cannot get the phase directly from intensity data. This is the phase problem of X-ray

crystallography. Two processes have been devised to solve this phase problem, and they are the Patterson method and Direct methods.

The Patterson method involves using a Fourier summation that results in an electron density map similar to that of the electron density maps that result from a Fourier transform. The Patterson method gives rises to peak heights of the largest atoms in the unit cell first and once you locate one atom with enough confidence, other atoms can be located via the Patterson map. Other Fourier methods can be used to minimize the R-factor by least squares refinement and you may be able to detect previously undetected light atoms like hydrogen. The Patterson method is most successful when there are a few heavy atoms in the structure, relative to a larger number of light elements. The Direct methods approach uses statistical probabilities by choosing three reflections whose phases are not known and can be positive or negative. These three reflections have eight possible combinations and for each combination the phases of each reflection can be predicted. These phase predictions result in an electron density map called an *E-map* that can be used to determine atomic positions. Once the structure is solved using one of these two methods, it is refined using a least-squares method until the calculated and experimental intensities converge as closely as possible.

Bond Valence Sum Theory

The bond valence sum theory was derived from the concept of bond strength and was introduced by Pauling in 1947, but was first adapted to oxides in the 1951 by Bystrom and Wilhemi and also in 1963 by Zachariasen³. The use of

bond valence parameters can estimate bond lengths in crystals to a very close approximation and has therefore become a very useful tool in the solid state chemistry world. More recently, bond valence parameters have been calculated and displayed in papers by Brown in 1981 and another by Brown with Altermatt in 1985¹². A subsequent paper in 1991²⁰ by Brese and O'Keeffe provided more parameters, and uses the most common bond valence expression $v_{ij} = \exp[(R_{ij} - d_{ij})/b]$, where v_{ij} is the valence of a bond between two atoms i and j , d_{ij} is the bond length, R_{ij} is the experimentally determined bond valence parameter, and b is a "universal" constant equal 0.37 \AA ¹³. The paper by Brese and O'Keeffe delivers 969 bond valence parameters, R_{ij} , by manipulating the above equation to give the formula $R_{ij} = b \ln [V_i / \sum_j \exp(-d_{ij}/b)]$, where V_i is the oxidation state of cation i . The parameters that were reported had an accuracy of $\pm 0.02 \text{ \AA}$ because, in general, bond lengths can rarely be determined with an accuracy greater than 0.01 \AA . In all, the Brese/O'Keeffe paper delivers bond valence parameters of 66 cations to be paired with 12 anions with less than a 3% error for most of the parameters. The highest error occurs between the pairing of atoms with alternating high-spin and low-spin states and this error is only 14%. Overall, bond valence theory is a very powerful tool for checking X-ray structures, and is better than using the sums of ionic radii to predict bond lengths in crystal systems and may be useful in determining coordination numbers if there is significant bonding interaction between pairs of atoms.

CHAPTER II

PEROVSKITES AND NITRIDE FLUORIDES

Perovskite Background

Perovskite-related materials are amongst the most abundantly studied of all inorganic crystalline solids, and will play an important role in this thesis as well. The perovskite structure is of the general formula ABX_3 where X is oxygen and A and B are metals with oxidation states that add up to +6, or X is fluorine and A and B are metals with their oxidation states adding up to +3. The ideal perovskite-type structure has a primitive cubic unit cell with the oxygen atoms centered on the edges or faces of the unit cell, with atoms of one of the metals centered on the corners atoms of the other metal in the center of the unit cell, all of which can be seen in Figure 2.1. In an ideal cubic perovskite, ABX_3 , in which all atoms are just touching, the cell edge is given by $(2R_X + 2R_B)$, where R is the radius of X and B respectively. The diagonal of the unit cell is 1.414 times the cell edge and could be represented as $(2R_X + 2R_A)$. An ideal cubic perovskite lattice should then obey the following formula:

$$R_X + R_A = 1.414(R_X + R_B)$$

However, these structures are not always ideal and allow for a tolerance factor, t , to be applied to the above formula to give:

$$R_X + R_A = t * 1.414(R_X + R_B).$$

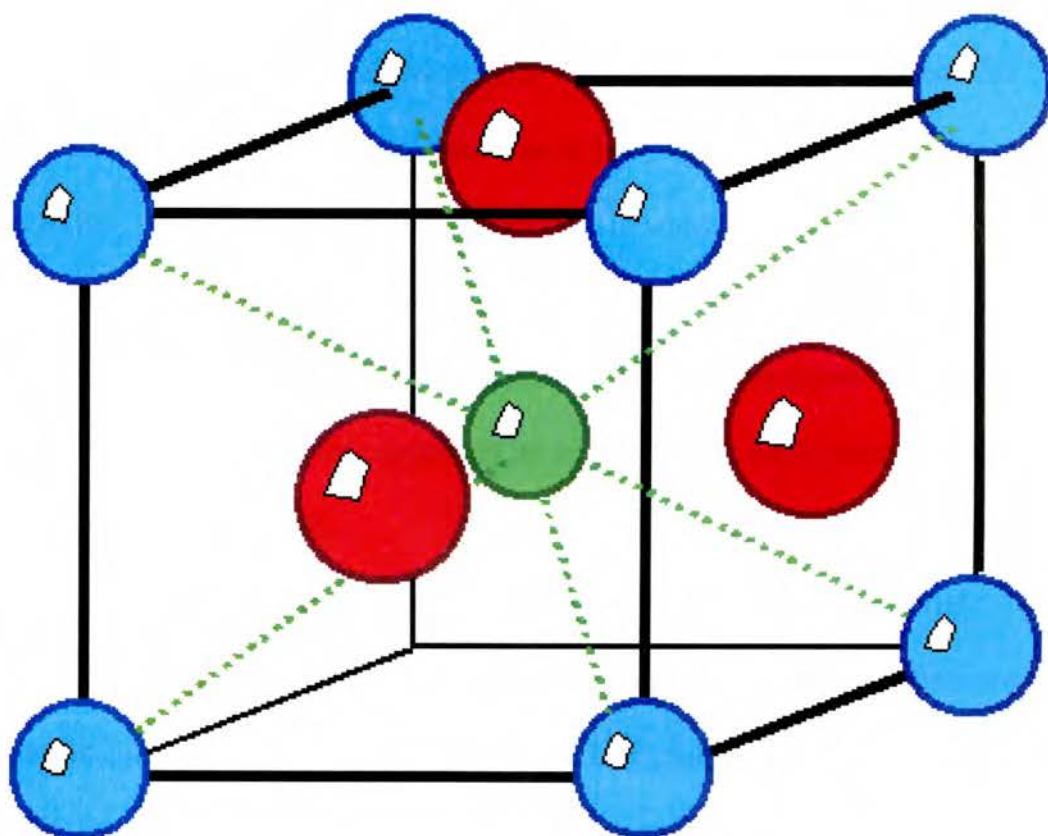


Figure 2.1 A Perovskite Structure. The blue atoms represent a metal like calcium, oxygen or fluorine is in red, and something like titanium is in green²⁹.

This tolerance factor represents the degree of variation of the atoms in the perovskite structure. Compounds with the perovskite structure generally have a tolerance factor between 0.80 and 1.00, as is evidenced by the number of different perovskite compounds in Table 2.1. However, the ideal perovskite structure appears only to be possible in compounds with a tolerance factor between 0.90 and 1.00. Compounds with a tolerance factor below 0.90, like perovskite itself (CaTiO_3 , $t = 0.81$), adopt a deformed structure in which the atoms are slightly displaced from their ideal positions, thereby reducing the symmetry of the structure. Thus, many of the deformed perovskite structures appear to have orthorhombic or monoclinic symmetry, as opposed to the cubic symmetry of the ideal perovskite unit cell.

Compounds with the perovskite structure hold a wealth of potential because of their useful magnetic and electrical properties and because there are almost endless possibilities for new compositions, including mixed anion compounds of the type discussed later. Dielectric properties of perovskite compounds, BaTiO_3 for example, are very important for their commercial applications as capacitors. They are also important in trying to understand the large change in resistivity that some of these compounds undergo when exposed to a medium or small magnetic field. This phenomenon, known as the colossal magnetoresistance effect, is very interesting because materials that exhibit this effect have possible uses in magnetic storage devices. Many metal oxides and other inorganic solids exhibit magnetoresistance, but only to the point where the resistivity of the compound changes by 10-20%. However, when a small magnetic

Table 2.1 Summary of Some Perovskite Compounds and Their Tolerance Factors²

Compound	Tolerance Factor	Compound	Tolerance Factor
KNbO_3	(0.92)	CaSnO_3	(0.80)
NaNbO_3	(0.80)	SrSnO_3	(0.84)
CdTiO_3	(0.81)	BaSnO_3	(0.92)
CaTiO_3	(0.81)	LaMnO_3	(0.87)
SrTiO_3	(0.86)	LaFeO_3	(0.88)
BaTiO_3	(0.93)	LaCrO_3	(0.88)
CaZrO_3	(0.77)	KMgF_2	(0.95)
SrZrO_3	(0.81)	KZnF_2	(0.91)
BaZrO_3	(0.88)	KNiF_2	(0.93)

field is applied to certain perovskite-related materials such as the Ca/La manganites, they experience a change in electrical resistance by about an order of magnitude. This effect will hopefully be able to be studied and understood more fully through the examination of electrical and metallic properties of the proposed mixed metal nitride-fluoride.

Preparing a mixed metal nitride fluoride of a perovskite is not only beneficial from a practical standpoint, but also from a crystal chemical perspective because structure of this composition have never been made. The synthesis of the proposed compound CaMnNF_2 would be advantageous in comparing nitride fluoride compounds to their oxide counterparts. One of the effects that sparks interest is the fact that manganese in the proposed CaMnNF_2 could be distorted in an octahedral environment simply due to mixed anion coordination, and such distortions in general can yield useful electrical properties. In addition, the Mn atoms in this compound would be present as the d^4 , Mn^{3+} ion and would be subject to Jahn Teller distortions. CaMnO_3 , on the other hand, has Mn^{4+} present, which is d^3 and doesn't have Jahn-Teller distortions. Such distortions in oxides are thought to play an important role in the colossal magnetoresistance effect. All these interesting properties of oxide materials make the study of their nitride fluoride analogs very intriguing.

Nitride-Fluoride Background

Inorganic nitride-fluoride chemistry has been a relatively neglected area of study in solid state chemistry, but there has been an increase in the interest of

these materials in recent years. One reason for this lack of activity may be that although the preparation of metal nitride fluorides appears to be simple from the reaction standpoint, in practice it is very tedious. Many of the reported nitride fluoride compounds are very air sensitive and the reactants must be mixed in an inert atmosphere, usually argon, followed by reaction with nitrogen gas in such a way so as to keep oxygen from reacting with the nitride fluoride product. One of the first studies on inorganic nitride-fluorides was reported in 1970 in the *Journal of Solid State Chemistry* by Sten Andersson⁴ on the Mg-N-F system. All three nitride fluorides that Andersson synthesized have rocksalt-related structures like their analogous oxide, MgO. Two of these phase were designated as L-Mg₂NF and H-Mg₂NF, the low and high temperature forms, respectively, where L-Mg₂NF reportedly has a structure intermediate between zincblende and rocksalt and the H-Mg₂NF has the rocksalt structure. The third phase, Mg₃NF₃, is related to that of MgO except that 1/4 of the magnesium atoms are empty in an ordered fashion. All of these structures were determined by X-ray powder diffraction and the data was analyzed by least squares crystal structure refinement calculations.

Powder samples of Ca₂NF, Sr₂NF and Ba₂NF have been reported by Ehrlich⁵ *et al*, and were classified as having the rocksalt structure of their oxide analogs through a qualitative study using the Guinier powder X-ray diffraction method. In addition to alkaline earth metal nitride fluorides, some transition metal nitride fluorides have also been reported. Among these are TiNF⁶, which has been shown to have the TiO₂ anatase-like structure. ZrNF was reported as a nitride fluoride but has since been reinterpreted as an oxy-nitride-fluoride and has a

compositely modulated structure⁷. Some other compounds like Zn_2NF , $TcNF$, $ThNF$ were reported by Marchand^{8,9,10} *et al.* but little or no structural data was reported. In addition to these three compounds, Bi_3NF_6 , Ce_3NF_6 , and Pr_3NF_6 have been reported in an investigation largely focused on the synthesis of N-F compounds through ammonolysis of ammonium fluorometalates^{11,12}. The research done at YSU has yielded five nitride-fluoride structures of the M_2NF type, where $M = Ca, Sr, \text{ and } Ba$, and an unpublished structure of $Ca_{1.26}Mn_{0.76}NF$ that is of the rocksalt-type lattice and is summarized in Table 2.2. The rocksalt phases for the $M = Ca, Sr, \text{ and } Ba$ had been previously reported but not well characterized, so quantitative structural analyses on the M_2NF compositions were done for the first time at YSU by using single-crystal X-ray diffraction. Three lattice structures of these nitride-fluoride analogs have been observed and are shown in Figure 2.2. The structures include the rocksalt-type in Ca_2NF analogs, tetragonal, which is exhibited by the $L-Mg_2NF$ type, and a new phase called "doubled-cubic" that was reported in Ca_2NF and Sr_2NF analogs. It is called doubled-cubic because the cell edges are double the length of the rocksalt structure due to N-F ordering along all three unit cell axes.

The interest in these structures has risen because there is much opportunity to make new compounds with structures related to analogous oxides, but with enhanced anion-induced properties. It is also of interest to compare these new materials to their oxide counterparts to learn more about the properties of the oxides themselves. As mentioned, several single metal nitride-fluorides have been

Table 2.2 Summary of Known M_2NF Compounds (bold-faced compounds characterized by YSU Wagner Group)

Oxide Analog (all rocksalt-type)	Doubled-cubic N-F analogs	Tetragonal N-F analogs	Rocksalt-type N-F analogs
MgO		L-Mg ₂ NF ⁴	
CaO	Ca₂NF¹⁶	L-Ca₂NF¹⁴	Ca ₂ NF ⁵ , Ca₂NF (This Study)
SrO	Sr₂NF¹⁵		Sr ₂ NF ⁵
BaO			Ba ₂ NF ⁵ , Ba₂NF¹⁷

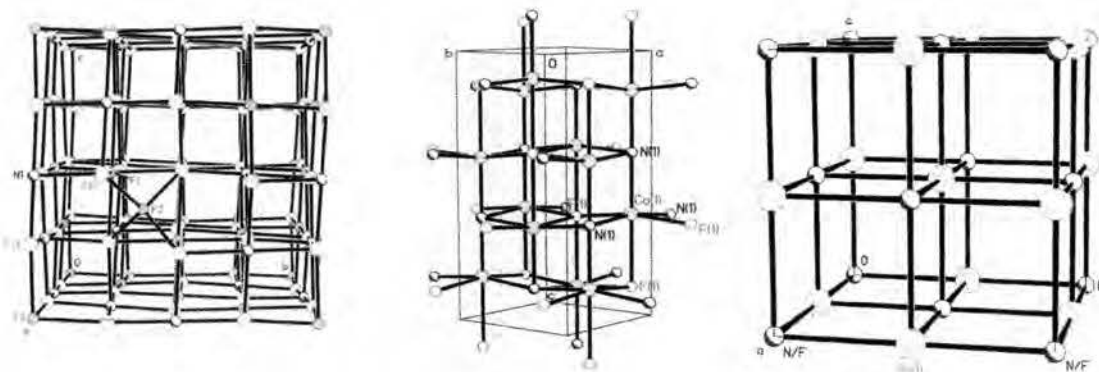


Figure 2.2 Three different reported structure types of compounds of M_2NF formula. From left to right is the doubled-cubic phase,¹⁶ the tetragonal phase,^{4, 14} and the rocksalt phase^{5, 17}.

prepared, but to date, no mixed metal inorganic nitride-fluoride or nitride-oxide-fluoride has been reported.

CHAPTER III

STATEMENT OF THE PROBLEM

There are two overall goals of this research. The first is to study air stability of nitride-fluorides as a function of oxygen content, and the second is to attempt to prepare mixed-metal nitride-fluorides or nitride-oxide-fluorides for the first time. Nitride fluoride compounds offer a wealth of possibilities in the solid state world because the introduction of the nitrogen and fluorine in place of oxygen maintains the average charge of the anions at -2, but the smaller band gap due to the lower electronegativity of nitrogen presents an advantage in terms of optical and electrical properties. The fact that they are often not air stable presents a problem in terms of practical applications. A proposed solution to the air stability problem is to introduce oxygen to the nitride-fluoride system. This first goal will be attained through investigation of the rocksalt-type $\text{Ca}_2\text{N}_x\text{O}_{2-2x}\text{F}_x$ system over a wide range of X. Single crystalline products will be targeted, and structure and cell parameters quantified through X-ray diffraction methods. Compositions will be estimated through analysis of cell parameters, assuming that CaO and Ca_2NF end members are both known. No single crystal studies of rocksalt-type Ca_2NF have been previously reported

The second goal is to prepare novel mixed metal N-F or N-O-F materials with potentially useful properties. Of particular interest in this project is the Ca-Mn-N-F and Ca-Mn-N-O-F systems since these materials could have important

magnetic properties similar to those observed in the (Ca, La)MnO₃ perovskite type compounds. Attempts in previous trials to obtain a mixed metal, mixed anion system have not yielded much success because of the purity of the reactants was questionable. Therefore, instead of using synthesized Ca₂NF, which may have unreacted starting material from its synthesis, other reaction routes will be used in order to guarantee purity of the reactants and increase the chances of success.

CHAPTER IV

METHODS AND MATERIALS

Crystal Mounting

Thanks to previous research done by other graduate students at Youngstown State University¹⁴, there weren't many different methods of crystal mounting methods to explore. One of the methods that failed involved gluing the crystal to a capillary, but either the glue was too thick and the crystal wouldn't diffract or there was not enough glue and the crystal would be exposed and would decompose. It is also possible that the crystal reacted with the glue. Ultimately, samples for this study were prepared for X-ray analysis by encapsulating the crystal in petroleum jelly and inserting it into a capillary tube about the same size of the crystal. Capillaries were made from glass pipettes by rolling a pipette over a flame from a Bunsen burner and when the glass is pliable enough, pulling the pipette apart rapidly to about arms length. It is very helpful to wear latex gloves during this process to help prevent your hands from slipping off the glass pipette when you begin to stretch it and pull it away from the flame. After the capillaries are made, they are cut down under an optical microscope so that the opening is roughly the same size as the crystal being mounted. Once a suitable capillary is prepared, it should be cut down to about an inch in length and fused into the brass pin that in turn will be inserted into the goniometer head. Wax or glue can be used to secure the capillary into the brass pin. To use wax, simply heat the brass pin

and then touch wax to the opening of the pin and melted wax fills the pin. While the wax is still liquid the capillary is inserted into the wet wax, centered, and the wax allowed to harden. Wax is preferred to glue because it is easier to reuse the pins with this method, but the capillary is still held firmly. At this point, the crystal can be mounted. To do this, the brass pin with the capillary is placed in the end of a rubber stopper because it is easier to maneuver the rubber stopper as opposed to the brass pin because the pin is quite small. The selected crystal will usually be immersed in petroleum jelly for protection from air, and can usually be scooped into the capillary with relative ease. If it doesn't go right in, you can use the edge of a small scalpel or razor blade to push it into the capillary. It is very important to make sure the capillary opening is roughly the same size as the crystal because if it's too big, the crystal can slide to the bottom of the capillary during the diffraction process and you will have to remount. In addition, if the capillary opening is too small, the crystal won't go in and it may temporarily rest perfectly on the tip of the tip of capillary, but it will probably fall off during the diffraction process. Once the crystal is mounted, the brass pin is transferred from the rubber stopper to the goniometer head and it is ready for X-ray analysis.

Single-Crystal Data Collection and Analysis

All but one data set for the single-crystal samples described in this thesis were collected on the SMART APEX CCD system at YSU and the data analyzed by the Bruker SHELXTL package, version 6.10. The targeted mixed-metal, mixed-anion single crystal, which turned out to be an oxide, was analyzed on site

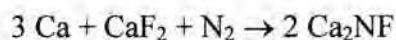
at YSU, but it didn't give enough high intensity data to solve the structure completely so synchrotron data was collected at the Advanced Light Source in Berkeley California, and that is the data that is described in this thesis.

CHAPTER V

EXPERIMENTAL RESULTS

Preparation of $\text{Ca}_2\text{N}_x\text{O}_{2-2x}\text{F}_x$ Compounds

The first preparation in this series of experiments was to reproduce previous results of Jack¹⁶ *et al.* and Nicklow¹⁴ *et al.* In both studies, single crystals of Ca_2NF were prepared using the following reaction:



Jack¹⁶ *et al.* produced a structure with a doubled-cubic lattice, which was a new result for this system, and Nicklow¹⁴ *et al.* produced single crystals of the L- Ca_2NF phase, which is isostructural to the L- Mg_2NF phase reported by Andersson⁴. For the current preparation, the mass of calcium used was 1.339 g, corresponding to 0.0343 moles of calcium. This was used to calculate the amount CaF_2 to be used (3 moles Ca:1 mole CaF_2) which turned out to be 0.671 g. The reactants were weighed and put into a nickel crucible in the presence of argon gas, concealed in a glove bag. The crucible was then placed in the reaction tube, which is in turn placed in the furnace and reacted according to the following program (R = Ramp function, L = Temperature level, D = Dwell function):

Step 1: R1: Step function; L1: 28°C; D1: 0.0 hours

Step 2: R2: 60°C/hr; L2: 1100°C; D2: 1.0 hour

Step 3: R3: 80°C/hr; L3: 200°C; D3: 2.0 hours

Switch from argon gas to nitrogen gas during step 3 dwell

Step 4: R4: 60°C/hr; L4: 1100°C; D4: 3.0 hours

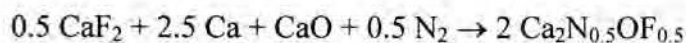
Step 5: R5: 20°C/hr; L5: 200°C; D5: 0.0 hours

Step 6: R6: Step function; L6: 28°C; D6: End function

It is not imperative to switch over to the nitrogen gas exactly during the dwell period of step 3 because the reactants will not react until the furnace gets back up to the temperature where the reactants will melt again. However, it is good practice to switch the gases as close to this time as possible, so before starting the reaction, the time that will elapse during each step was calculated in order to promptly switch the gases. The products of this reaction were a mixture of orange crystals and black/gray powder and they were immediately placed on a slide in the glove bag, with argon circulating the bag, and encased in petroleum jelly to prevent decomposition. The orange crystals were submitted for single crystal analysis and they produced the rocksalt-type Ca_2NF with $a = 4.9803 \text{ \AA}$.

Refinement results will be discussed in chapter 6.

The second preparation was an attempt to synthesize an N-O-F analog of calcium oxide with the intent to possibly eliminating the sensitivity to air of all the previously reported N-F compounds. The following reaction was used:



The mass of calcium used was 0.701 g, the mass of CaF_2 used was 0.273 g and the mass of CaO used was 0.392 g. It wasn't realized until after the reaction was done that this reaction is not balanced stoichiometrically in terms of oxygen content, so the reaction was in effect run with excess calcium present. For the product suggested, a coefficient of 2 should have been in front of the CaO and a

coefficient of 1.5 in front of the Ca. The same program was used for this preparation as for the previous experiment. The products were once again some orange crystals and black/grey powder, with the addition of yellow crystals. Once again, the products were immediately transferred from the nickel crucible to a microscope slide and encased in petroleum jelly while in a glove bag circulated with argon gas. Both the orange and yellow crystals were submitted for single crystal X-ray analysis with the data being collected at room temperature. The orange crystals turned out to be the same as in preparation 1, but the yellow crystals were slightly different. They were also of the rocksalt-type but had a cell edge of $a = 4.937 \text{ \AA}$, exactly the same as the reported powder sample of Ca_2NF by Ehrlich⁵ *et al* in 1970. This is interesting in that it suggests that Ehrlich's sample is actually a Ca-N-O-F phase. Refinement results are further discussed in chapter 6.

Since it appears that previously reported phases of Ca_2NF likely contained oxygen, the third and fourth preparations involved introducing a mixture of 95% N_2 and 5% H_2 gases as the reacting gases instead of just nitrogen, in an attempt to eliminate all present oxygen from the Ca_2NF reaction system. For this preparation the same reaction (3 moles Ca:1 mole CaF_2) was used and care was taken, as usual, to weigh and mix the reactants under argon. This reaction has proven to be very effective at producing Ca_2NF crystals, and therefore was not modified. The mass of calcium used was 0.420 g and the mass of CaF_2 used was 0.273 g and the reaction was run with an identical furnace program to the one used in the first preparation. This had a similar product yield as the previous reaction. There was a mixture of yellow and brown/orange crystals and what appeared to be some

unreacted starting material. These crystals were transferred to a microscope slide, encased in petroleum jelly and examined under a microscope. Many of the nicely colored crystals appeared to be multi-crystalline. The best way to describe these results is by thinking of a snowball. A snowball is made up of many individual snowflakes and that is how you can describe what happened here, many tiny crystals stick together to make what appears to be one big crystal. The approach to separating a multi-crystalline sample into single crystals is to try to shave off some of the smaller crystals so that you can get better data from X-ray diffraction analysis. The problem here was that the crystals that were separated from the bigger chunk of crystal were too small, and didn't diffract well enough to get unit cell parameters. In order to prepare larger crystals, the cooling rate was lowered so that there would be more time for larger crystals to possibly grow.

For the next preparation a slower cooling rate was applied to the reaction program in the third preparation. The same preparation was applied here and 0.460 g of calcium was used and 0.300 g of CaF_2 was used with the following reaction program:

Step 1: R1: Step function; L1: 28°C; D1: 0.0 hours

Step 2: R2: 60°C/hr; L2: 1100°C; D2: 1.0 hour

Step 3: R3: 80°C/hr; L3: 200°C; D3: 2.0 hours

Switch from argon gas to nitrogen gas during step 3 dwell

Step 4: R4: 60°C/hr; L4: 1100°C; D4: 3.0 hours

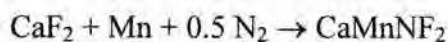
Step 5: R5: 10°C/hr; L5: 200°C; D5: 0.0 hours

Step 6: R6: Step function; L6: 28°C; D6: End function

It can be seen in step 5 that the cooling rate was lowered to 10°C/hr for this preparation, as opposed to 20°C/hr in the previous preparation. The only drawback to using a cooling rate of 10°C/hr during the crystal growth period is that reaction time is significantly lengthened. This particular reaction took just under six days to complete, which is almost two days longer than the previous reaction with a 20°C/hr cooling rate. However, this minor alteration turned out to be very significant. When the reaction was finished and the products examined under the microscope, there were still many multi-crystalline compounds, but the smaller crystals that were shaved off the main chunk were indeed bigger than in the previous preparation. Also, the products were once again orange and yellow crystals, but with a smaller amount of unreacted starting material. A few red crystals were found in the product mixture as well. These all turned out to be rocksalt-type phases, as discussed in chapter 6.

Proposed Synthesis of CaMnNF₂

The proposed reaction for the preparation of CaMnNF₂ target material was:



The reaction was done twice and at two different temperatures. The first time it was done at 1300°C because the melting points of CaF₂ and Mn, 1423°C and 1253°C respectively, suggesting that this would be a good temperature to melt the reactants completely to form a uniform reaction mixture for optimal single crystal growth. The reaction procedure involved weighing the reactants and placing them

in a nickel crucible while in an I²R glove bag, model S30-20H, under an argon gas atmosphere. After placing the reactants in a nickel crucible, the crucible was placed in a silica glass reaction tube, and subsequently placed into the ThermoLyne 59300 High Temperature Tube Furnace. The reactants were allowed to mix after melting by heating to 1300°C, holding for one hour, and then reducing the temperature to 200°C under an inert atmosphere of argon gas. Next, the atmosphere was switched from argon to nitrogen and the temperature was gradually raised back up to the reaction temperature of 1300°C where the reactants melted again. The mixture was held at this temperature for a period of three hours and then the temperature was reduced again but at a slower rate that allows for the growth of single crystals. Previous nitride-fluoride syntheses have used cooling rates ranging from 60°C/hr to 20°C/hr or slower. The slower cooling rates provide a better chance to form single crystals by allowing optimal conditions for nucleation and growth. In the case of this first reaction, the 1300°C reaction proved too much for the tube to handle. Although the tube cracked, a mixture of products were found ranging in color from black to dark blue to violet using the following program:

Step 1: R1: Step Function; L1: 28°C; D1: 0.0 hours

Step 2: R2: 80°C/hr; L2: 1300°C; D2: 1.0 hour

Step 3: R3: 80°C/hr; L2: 200°C; D3: 2.0 hours

Switch from argon to nitrogen gas between steps 3 and 4

Step 4: R4: 80°C/hr; L4: 1300°C; D4: 3.0 hours

Step 5: R5: 20°C/hr; L5: 200°C; D5: 0.0 hours

Step 6: R6: Step Function; L6: 28°C; D6: End Function

Since the reaction tube cracked and we were originally concerned about the effects of air on the products, the reaction was performed a second time. For the second preparation, the temperature was decreased so as to preserve the life of the reaction tube. The heating and cooling cycle under an inert atmosphere of argon gas was skipped in this second trial to decrease the heating time on the reaction tube. The reaction temperature was only taken up to 1000°C so single crystals were not expected since it was anticipated that insufficient melting would occur to get single crystals to grow, and thus, a powder phase was targeted for this preparation. During the preparation of the reactants in the crucible, extra care was taken to make sure the reactants were mixed as thoroughly as possible so as to make the reaction mixture homogeneous. The cooling rate was also increased, since a powder phase was expected. Surprisingly, some very small violet/purple crystals were formed along with some green crystals. The reaction tube was not compromised on this run so the green and violet crystals were submitted for single crystal analysis. The following program was used in this second reaction:

Step 1: R1: Step Function; L1: 28°C; D1: 0.0 hours

Step 2: R2: 60°C/hr; L2: 1000°C; D2: 8.0 hours

Step 3: R3: 40°C/hr; L3: 200°C; D3: 0.0 hours

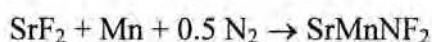
Step 4: R4: Step Function; L4: 28°C; D4: End Function

The green crystals turned out to be manganese oxide, but the violet/purple crystals were of interest. These crystals underwent single crystal X-ray analysis at YSU

but the crystals didn't produce enough data so they were sent to the Advanced Light Source at Berkeley for synchrotron analysis. The data that was received gave an orthorhombic lattice similar to brownmillerite and refined well with an apparent formula of $\text{Ca}_2\text{Mn}_2\text{N}_2\text{O}_2\text{F}$. The source of oxygen in this system was likely due to the silica reaction tube. As discussed in chapter 6, however, the compound actually turned out to have the composition $\text{Ca}_2\text{Fe}_2\text{O}_5$.

Attempted Synthesis of SrMnNF_2

After the success of getting single crystals from the previous system, other attempts were made to use other group 2 cations. The first attempt was to model the reaction used in the Ca-Mn system but to substitute strontium for calcium and so the reaction was as follows:



With the melting points of manganese being 1253°C and SrF_2 at 1450°C , the reaction was run at 1000°C because the Ca-Mn system resulted in single crystals at this reaction temperature. The reactants were weighed and mixed in the nickel crucible in an inert atmosphere of argon gas while confined to a glove bag. The nickel crucible was then placed in the reaction tube and the following furnace program was used for the first attempt:

Step 1: R1: Step Function; L1: 28°C ; D1: 0.0 hours

Step 2: R2: 60°C/hr ; L2: 1000°C ; D2: 8.0 hours

Step 3: R3: 40°C/hr ; L3: 200°C ; D3: 0.0 hours

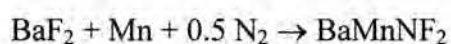
Step 4: R4: Step Function; L4: 28°C ; D4: End Function

For this reaction, 0.455 g of manganese was used and 1.052 g of SrF₂ was used, and the final product consisted of a mixture of green and orange products. There were some suitable green crystals but these were most likely manganese oxide as found in the product mixture from the Ca-Mn reaction discussed above. The orange products were mostly in powder form and there were no suitable single crystals. Because of this result, another reaction was run with a slower cooling rate to give the reactants more time to grow appropriately sized single crystals.

The second reaction program in this system was the same as the above program, but with a cooling rate of 20°C/hr in Step 3. This slower cooling rate didn't appear to have any effect on single crystal growth since the products of this reaction were basically the same. There didn't appear to be any suitable single crystals for X-ray diffraction and this system was not explored much further. Future studies of this system could reveal more success if reaction temperatures are higher than 1000°C, but not too high so as to ensure the integrity of the reaction tube, and usage of slower cooling rates.

Attempted Synthesis of BaMnNF₂

After briefly exploring the possibility of the Sr-Mn system, barium was substituted for strontium in the same manner that strontium replaced calcium. For this new preparation, the following reaction was used:



For this preparation, the reaction temperature was taken up to 1100°C to ensure the melting of the reactant mixture, since BaF₂ has a melting point of 894°C. The

reactants were weighed and mixed in the nickel crucible where the mass of BaF_2 used was 0.225 g and 0.395 g of manganese was used. All of this was done in the glove bag in the presence of argon gas, followed by insertion of the crucible into the reaction tube and the tube subsequently being inserted into the furnace with the following reaction program:

Step 1: R1: Step function; L1: 28°C; D1: 0.0 hours

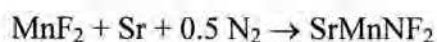
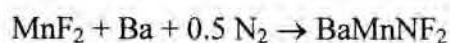
Step 2: R2: 60°C/hr; L2: 1100°C; D2: 8.0 hour

Step 3: R3: 20°C/hr; L3: 200°C; D3: 0.0 hours

Step 4: R6: Step function; L6: 28°C; D6: End function

It may be possible to use a different reaction program for this system where reactants are first melted under argon, but single crystals of green and orange colors were produced from this first preparation anyway. Once again, the green crystals were most likely manganese oxide, but the orange crystals were quite prominent and seemed very promising. However, after numerous attempts to obtain single-crystal data on a number of different crystals of appropriate size, it was concluded that these crystals were amorphous because they didn't diffract.

Other possible routes of synthesis for these systems could use the following reactions:



Using these reactions would allow you to melt the reactants under argon prior to reacting with nitrogen. This synthetic method assures complete mixing of the reactants and since all of these reactants have melting points below 1000°C, you

can have lower reaction temperatures and preserve the life of the reaction tube a little longer. Also, it may be advantageous to try these syntheses with a mixture of nitrogen and hydrogen gas. The data of the Ca-N-O-F system described previously shows that reacting with a 95%N₂/5%H₂ mixture results in basically ideal Ca₂NF. However, it may be necessary to have oxygen present to stabilize and produce these mixed metal, mixed anion systems.

CHAPTER VI

DISCUSSION

Ca₂N_xO_{2-2x}F_x System

The most significant result in the study of the Ca-N-O-F system is that previously reported rocksalt-type Ca₂NF compounds by Ehrlich⁵ *et al.* and Galy¹³ *et al.* appear to be N-O-F materials. This was revealed by an apparent synthesis of pure Ca₂NF in the presence of a mixture of N₂ and H₂ gases. The X-ray analysis of the Ca₂NF crystals from these syntheses gave some very significant results. As was previously mentioned, Ehrlich reported a Ca₂NF powder sample with the cell parameter of $a = 4.937 \text{ \AA}$. This number is significant because the first synthesis in this area of the research was designed as an attempt to introduce oxygen into the cell composition in an effort to make Ca₂NF more air stable and it produced a unit cell with $a = 4.937 \text{ \AA}$ that was obtained from X-ray data collected at room temperature. Also, subsequent research has yielded four other phases with cell parameter a larger than 4.937 \AA , including one with $a = 4.9841 \text{ \AA}$. Thus, one can conclude that the Ehrlich powder phase contained oxygen.

Galy¹³ *et al* used a formula similar to the following to correlate the cell edge, a , of rocksalt-type Ca₂N_xO_{2-2x}F_x to the relevant ionic radii, R_{ion} :

$$a_{Ca_2N_xO_{2-2x}F_x} = 2\{R_{Ca^{2+}} + [(xR_{N^{3-}} + (2-2x)R_{O^{2-}} + xR_{F^-})/2]\}$$

They assumed their reported phase with $a = 4.965 \text{ \AA}$ to be oxygen free Ca₂NF, and used this cell parameter along with ionic radii reported by Ahrens²¹ for Ca²⁺ and

F⁻ to calculate the apparently unavailable ionic radius for N³⁻. Today, the most commonly used values of ionic radii by solid state chemists are from crystal radii reported by Shannon²². These values take into account ionic charge, coordination number, and other factors. Unfortunately, no value is reported for R_{N³⁻} in six-fold coordination, which happens to be the anion coordination in rocksalt, and this value was calculated using the Galy approach. This is done, assuming the Ca₂NF phase reported here with $a = 4.9841$ is oxygen free, by employing the following equation with Shannon radii²² values of $R_{Ca^{2+}} = 1.14 \text{ \AA}$ and $R_{F^{-}} = 1.19 \text{ \AA}$:

$$a_{Ca_2NF} = 2\{R_{Ca^{2+}} + [(R_{N^{3-}} + R_{F^{-}})/2]\}$$

This produces a value of $R_{N^{3-}} = 1.51 \text{ \AA}$ and using this value in accordance with $R_{O^{2-}} = 1.26 \text{ \AA}$ and the $a_{Ca_2N_xO_{2-2x}F_x}$ equation given previously above, it is possible to qualitatively predict the compositions of our compounds in the Ca₂N_xO_{2-2x}F_x system. When using the first formula mentioned above, it should be apparent that x increases linearly from CaO, where $x = 0$, to Ca₂NF, where x is assumed to be 1. It is also worth noting that since Ca₂NF is assumed to be given by the sum of crystal radii, for consistency purposes, the sum of crystal radii was also used to obtain the cell parameters of the other end member in this system, CaO. Table 6.1 lists unit cell parameters, estimated compositions and other data for the Ca₂N_xO_{2-2x}F_x compounds prepared in this study and elsewhere. It is always a possibility that some oxygen is present in the phase of Ca₂NF with $a = 4.9841 \text{ \AA}$, but it certainly can be stated that that structure has the smallest amount of oxygen, if any at all, present relative to all of the previously reported structures.

Table 6.1: Compositional Estimates of $\text{Ca}_2\text{N}_x\text{O}_{2-2x}\text{F}_x$ Phases

Exp. Cell Parm., a, Å	X	Formula	Color	Comments
4.80	0	CaO	white	Estimated a = 4.80 Å from sum of radii
*4.937	0.744	$\text{Ca}_2\text{N}_{0.74}\text{O}_{0.52}\text{F}_{0.74}$	yellow	CaO reactant, room temp X-ray data
4.9570(10)	0.853	$\text{Ca}_2\text{N}_{0.85}\text{O}_{0.30}\text{F}_{0.85}$	red	Ca & CaF_2 in N_2/H_2 ; qtz. tube is oxygen source
4.965(7)	0.896	$\text{Ca}_2\text{N}_{0.90}\text{O}_{0.20}\text{F}_{0.90}$	yellow	Prepared by Galy ¹³ <i>et al.</i>
4.9803(6)	0.979	$\text{Ca}_2\text{N}_{0.98}\text{O}_{0.04}\text{F}_{0.98}$	orange	Ca & CaF_2 in N_2/H_2 ; qtz. tube is oxygen source
4.9841(13)	1.000	Ca_2NF	yellow	Ca & CaF_2 in N_2/H_2 batch

*Same cell parameter reported by Ehrlich *et al.*⁵ for their Ca-N-O-F phase

In conclusion, it would appear as though the preparations discussed previously in this thesis have possibly produced the first pure rocksalt-type Ca_2NF single crystal sample. The evidence laid down here also calls into question previous studies of reported N-F compounds as they most likely have some oxygen. This research also opens up some new avenues of research on this topic. It begs whether or not certain physical properties, such as color or air stability, can be tuned based on the amount of oxygen in the system. The $\text{Ca}_2\text{N}_x\text{O}_{2-2x}\text{F}_x$ system does not appear to be more air stable with addition of oxygen into the system because all of the compounds prepared throughout this study degraded within two weeks of creation, even when stored immediately after synthesis in petroleum jelly. The range of colors seen throughout numerous preparations of compounds in this system does not appear to follow any discernable pattern. Further explanations of these unanswered questions are very desirable and will be sought in the future.

$\text{Ca}_2\text{Fe}_2\text{O}_5$ System

The target of this part of the research was to synthesize CaMnNF_2 , a mixed metal N-F compound with a perovskite like structure. It was originally believed that this target material was prepared upon looking at the X-ray data with lattice parameters of $a = 5.437 \text{ \AA}$, $b = 5.577 \text{ \AA}$, and $c = 14.703 \text{ \AA}$. The a and b parameters were very similar to the lattice parameters of CaMnO_3 , but the c parameter for the new compound was roughly twice that of CaMnO_3 . Further analysis of the structure

was obtained by sending the crystal to the Advanced Light Source at Berkeley for high intensity synchrotron data. This data revealed the crystal to have lattice parameters of $a = 14.736 \text{ \AA}$, $b = 5.440 \text{ \AA}$, and $c = 5.603 \text{ \AA}$. The structure had an orthorhombic lattice and what appeared to be two distinct manganese sites and three anion sites. There was a lot of high intensity data and bond valence theory, as well as refinement data (see Appendix for refinement summary table) where $R1 = 0.0394$, suggested that the compound that was formed was $\text{Ca}_2\text{Mn}_2\text{N}_2\text{O}_2\text{F}$. An interesting observation of this structure revealed that the coordination of the manganese ions in this structure were similar to that of the orthorhombic compound $\text{Ca}_2\text{Mn}_2\text{O}_5$ ($a = 5.432 \text{ \AA}$, $b = 10.242 \text{ \AA}$, $c = 3.742 \text{ \AA}$), but the anion ordering and the lattice parameters more resembled brownmillerite, $\text{Ca}_2\text{Fe}_2\text{O}_5$ ($a = 5.425 \text{ \AA}$, $b = 5.598 \text{ \AA}$, $c = 14.768 \text{ \AA}$). In order to verify the composition, and especially the presence of nitrogen and fluorine, the sample was submitted to Materials Research Labs, Inc (MRL). The crystal composition of the sample was verified by X-ray microanalysis using a scanning electron microscope at MRL and, surprisingly the data revealed the composition of the compound to be $\text{Ca}_2\text{Fe}_2\text{O}_5$. After refining the structure with this new formula, the $R1$ value was 0.0364 for all data (see Appendix B for refinement summary table) as opposed to $R1 = 0.0394$ for all data in the best refinement of the crystal as $\text{Ca}_2\text{Mn}_2\text{N}_2\text{O}_2\text{F}$. Since manganese and iron have similar atomic sizes and scattering factors, bond valence theory and the synchrotron data by itself could not determine the exact composition of the sample. These crystals of $\text{Ca}_2\text{Fe}_2\text{O}_5$ were obviously created from some iron that must have contaminated the synthetic system.

A structure plot for $\text{Ca}_2\text{Fe}_2\text{O}_5$ is shown in Figure 6.1 and it can be seen that the O(3) atoms seem to be positioned as pairs, very near one another. This was originally assigned as a fully occupied 8h site, which has two sites 1.13 Å apart, and gives a formula of CaFeO_3 or $\text{Ca}_2\text{Fe}_2\text{O}_6$. The position was reassigned with 50% occupancy to obtain the correct composition of $\text{Ca}_2\text{Fe}_2\text{O}_5$. The Fe(2) atom was originally assigned by SHELXTL to the 4e position, which is the location shown for the atom in figure 6.1. However, significant improvement in the refinement was achieved by reassigning Fe(2) to a 50% occupied 8h position. This essentially splits the Fe(2) site between two positions that are located 0.242 Å from either side of the 4e site, directly along the *b*-axis. The resulting environment of the Fe(2) atom is shown in Figure 6.2. The Fe(2) site plays an important role in the crystal chemistry of brownmillerite related $\text{Ca}_2\text{Fe}_2\text{O}_5$ because the orientation of the tetrahedral chains in each Fe(2) layer depends on which of the two nearby 8h sites is filled in any given coordination sphere. This is further discussed below.

After determining the structure of the prepared crystalline compound, a literature search was done to see if this structure had been characterized. A similar structure has in fact been characterized,²⁴ but it exists only at high temperatures, ~ 1000 K, and there are subtle differences in both the arrangement of the tetrahedral layers in the unit cell and the lattice parameters. Table 6.2 compares unit cell data for the literature phase vs. the phase discussed in this thesis. The lattice parameters are nearly identical but the slightly smaller cell of the compound in this thesis can be accounted for by the fact that the X-ray data used to determine

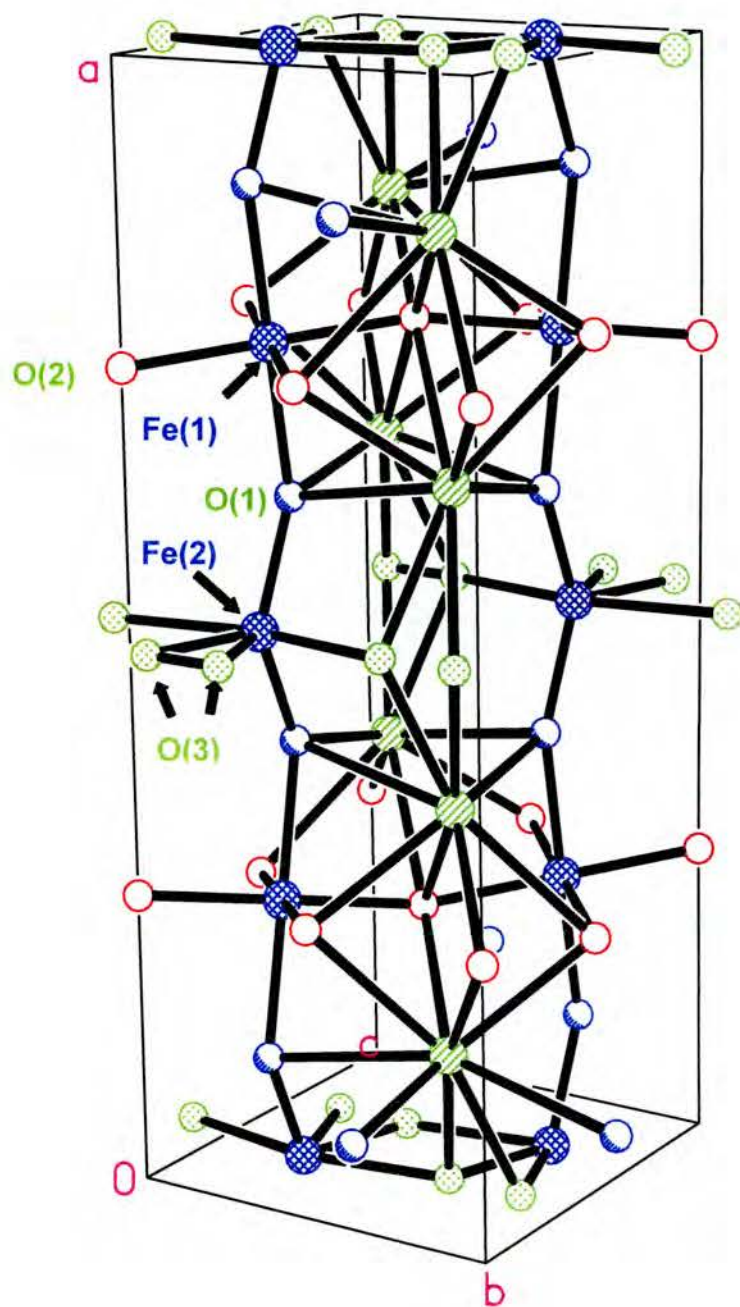


Figure 6.1 Ball and Stick Refinement of $\text{Ca}_2\text{Fe}_2\text{O}_5$

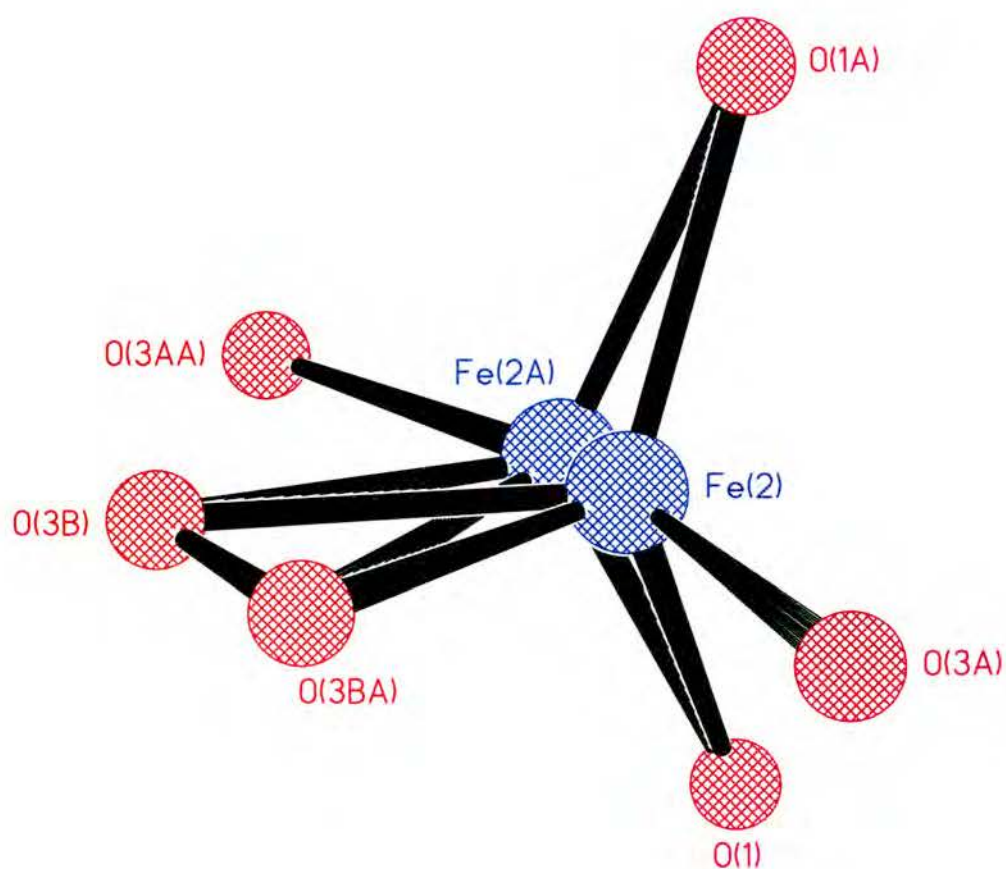


Figure 6.2 Fe(2) and O(3) 50% Occupied Environment

Table 6.2. Comparison of $\text{Ca}_2\text{Fe}_2\text{O}_5$ Structural Data for Literature vs. This Study

Literature Material ²³	Material From This Study
<p>Space Group.: Imma</p> <p>Unit Cell Parameters: a = 5.4931 Å b = 15.038 Å c = 5.6511 Å</p> <p>X-ray data collected at 1100 K</p> <p>Atomic positions: Ca(8h); Fe1(4b); Fe2(8i), O1(8g); O2(8h); O3(8i)</p>	<p>Space Group.: Imma</p> <p>Unit Cell Parameters: a = 14.7357 Å b = 5.4397 Å c = 5.6033 Å</p> <p>X-ray data collected at 273 K (accounts for the relatively smaller cell parameters), R1 = 0.0364 for all data</p> <p>Atomic positions (see Appendix) identical to literature positions except for shift in origin</p>

the parameters was collected at 273 K as opposed to 1100 K for the literature compound. In addition, the a and b axes are differently oriented when comparing the two compounds. In the literature compound, the b -axis is the long axis and in our compound, the a -axis is the long axis. These subtle differences point out the interesting crystal chemistry of this system, as indicated in Figure 6.3. Both compounds have an a -glide plane perpendicular to the c axis with reflection occurring in the a - b plane. Translation occurs via the a -axis in both structures, but because the a -axes are differently oriented in the two compounds, the translation occurs along the short axis in the literature compound and along the long axis in our compound. These glide plane differences are related to the different orientations of the tetrahedral chains of FeO_4 involving the Fe(2) and O(3) positions that are 50% occupied. As noted from Figure 6.2, the atoms that are placed into these two positions have two different orientations to choose from and thus, create two different tetrahedral environments of iron and oxygen atoms. Based upon whether the Fe(2) or Fe(2A) position is chosen will determine if a left-handed or a right-handed tetrahedral chain is generated, as indicated in Figure 6.4. These tetrahedral chains alternate throughout both structures but in very different ways because of the differing glide translations in these two structures. As previously mentioned, both structures translate along the a -axis but in the literature structure, the a -axis is the short axis and in our structure, the a -axis is the long axis. This means that our structure must have alternating layers of left-handed and right-handed chains along the long a -axis. As depicted in Figure 6.5, what is observed when looking at the structure along the b -axis with the a -axis

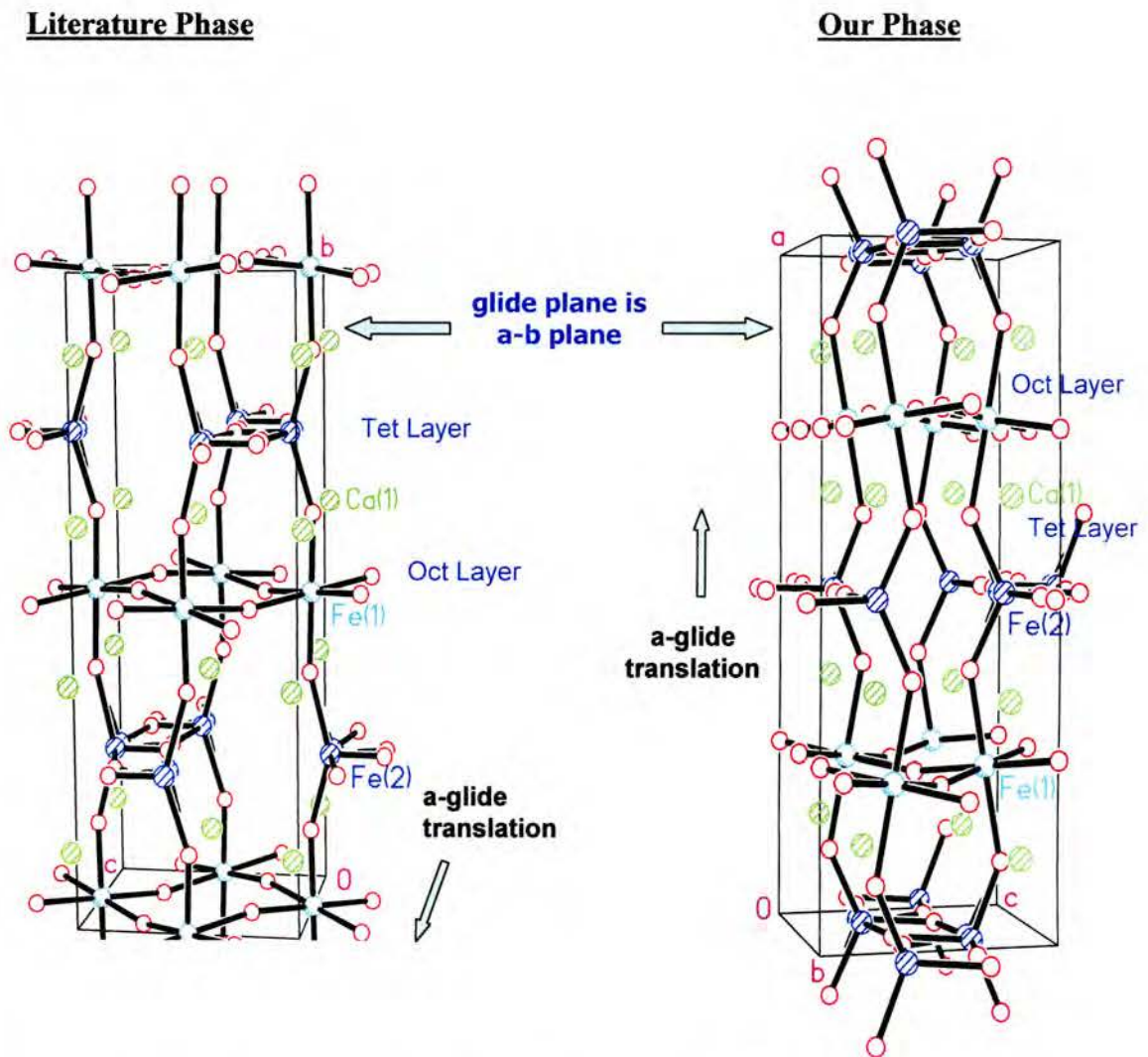
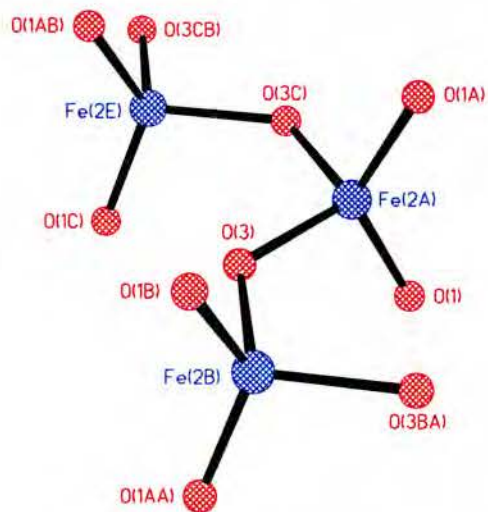
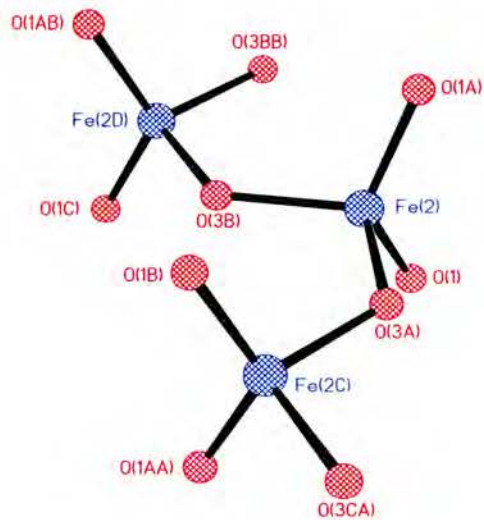


Figure 6.3 Comparison of Reported Literature Phase and Our Experimental Phase



Left-Handed Chain



Right-Handed Chain

Figure 6.4 Right and Left Handed Chains of FeO_4 . The choice of which position, Fe(2) or Fe(2A), to put Fe in at the mid chain determines whether the chain is left-handed or right-handed.

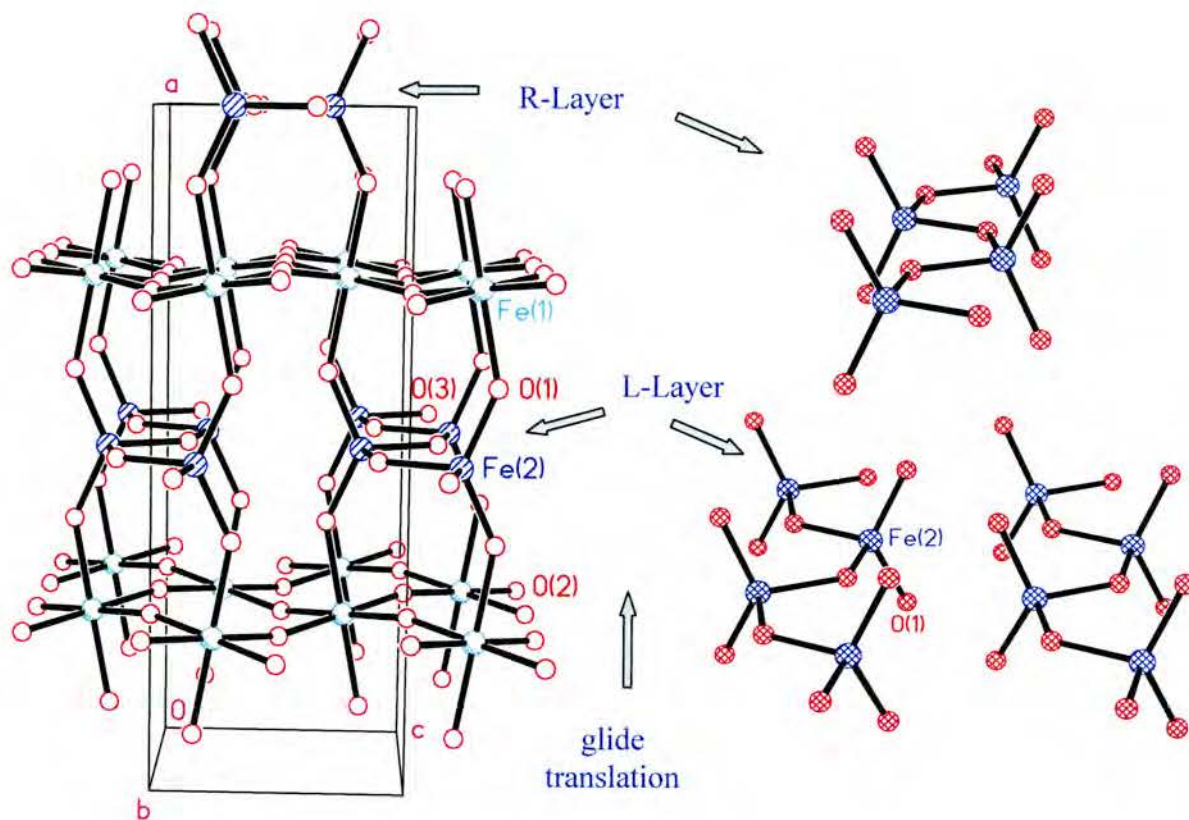


Figure 6.5 Orientation of the Fe(2) Chains in the Unit Cell

pointing up is the presence of only left-handed chains in one layer and right-handed chains in the layers above and below it. The literature structure, as seen in Figure 6.3, differs in that when looking at the structure along the a -axis, the long axis is now the b -axis and because of the orientation of the glide translation, there are now layers of alternating left-handed and right-handed tetrahedral chains within each layer, as opposed to layers that only contain left handed or right-handed chains as in our structure. In other words, the main difference between the two structures is that the glide translation occurs parallel to the tetrahedral layers in the literature case, but perpendicular to them in this case. This new structure is important because, although the composition is not different, the orientations of the atomic positions within the unit cell are. Also, this particular structure is stable at room temperature, whereas the literature structure is stable at around 1000 °C. As far as we know, this is the first observation of the $Imma$ phase at room temperature with alternate -LLL- and -RRR- tetrahedral layers. Usually, a $Pnma$ structure is observed having well ordered -LR- layers²³. In many brownmillerite type compounds, the tetrahedral chains can undergo a periodic ordering. For example, in the literature phase²³ referred to above, a periodic ordering of -LRLRLRLRR- was found in the tetrahedral layers. Such arrangements can lead to modulations, or long range ordering, in the lattice and the periodicity of a modulation will be proportionate or disproportionated with the underlying subcell lattice.

REFERENCES

1. DiSalvo, F.J., "Solid State Chemistry", *Solid State Comm.*, **102**, 79-85, (1997).
2. West, Anthony R., *Basic Solid State Chemistry*, John Wiley and Sons, New York, (1984).
3. Douglas, Bodie E., McDaniel, Darl H., and Alexander, John J., *Concepts and Models of Inorganic Chemistry*, Wiley, New York, (1983).
4. Andersson, S., "Magnesium Nitride Fluorides", *J. of Solid State Chem.*, **1**, 306-309, (1970).
5. Ehrlich, P., Linz, W., and Seifert, H., "Nitridfluoride der Schweren Erdalkalimetalle", *Naturwissenschaften*, **58**, 219-220, (1971).
6. Wustefeld, C., Vogt, T., Lochner, U., Strahle, S., and Fuess, H., "Synthesis of TiNF and Structure Determination by Powder Diffraction using Synchrotron Radiation", *Angew. Chem. Int. Ed. Engl.*, **27**, 929, (1971).
7. Stolz, C., Ramesha, P., Piccoli, B., Toby, B.H., and Eichhorn, B.W., "A_{0.3}ZrNF_{1.3} Phases (A = Na, K) with layered ZrNCl-type Structures Prepared by Anion Methathesis", *Chem. Mater.*, **17**, 5291-5296, (2005).
8. Marchand, R., and Lang, J., Zn₂NF, *Materials Research Bulletin*, **6**, 845-851, (1971).
9. LaVarle, Steele and Smith, TcNF, *J. Inorg. Nucl. Chem.*, **28**, 260, (1966).
10. Juza and Sievers, Z., ThNF, *Z. Anorg. Allg. Chem.*, **363**, 258, (1968).
11. Hofmann, M., Schweda E., Strahle, J., Laval, J.P., Frit, B., and Estermann, M.A., "Synthesis and Structure of Bi₃NF₆ – A Member with N=3 of the Vernier Phases M_NX_{2N+1}", *J. of Solid State Chem.*, **114**, 73-78, (1995).
12. Vogt, T., Schweda E., J., Laval, J.P., and Frit, B., "Neutron Powder Investigations of Praseodymium and Cerium Nitride Fluoride Solid Solutions", *J. of Solid State Chem.*, **83**, 324-331, (1989).
13. Galy, J., Jaccou, M., and Andersson, S., "Nitrofluoride, Ca₂NF. Oxy-nitrofluorinated Solid Solutions Ca₂O_{2x}N_{1-x}F_{1-x}", *C.R. Acad. Sc. Paris*, **272**, 1657, (1971).

14. Nicklow, R., Wagner, T., and Raymond, C., "Preparation and Single-Crystal Structure Analysis of Ca_2NF ", *J. of Solid State Chem.*, **160**, 134-138, (2001).
15. Wagner, T., "Preparation and Single-Crystal Structure Analysis of Sr_2NF ", *J. of Solid State Chem.*, **169**, 13-18, (2002).
16. Jack, D.J., Zeller, M., and Wagner, T.R., "Doubled-cubic Ca_2NF ", *Acta Cryst. C*, **C61**, i6-i8, (2005).
17. Seibel, H., and Wagner, T., "Preparation and Crystal Structure of Ba_2NF ", *J. of Solid State Chem.*, **177**, 2772-2776, (2004).
18. Ramirez, A.P., "Colossal Magnetoresistance", *J. Phys.: Condens. Mater.*, **9**, 8171-8199, (1997).
19. Brown, I.D., and Altermatt, D., "Bond-Valence Parameters Obtained from a Systematic Analysis of the Inorganic Crystal Structure Database", *Acta Cryst. B*, **B41**, 244-247, (1985).
20. O'Keeffe, M., and Brese, N.E., "Bond Valence Parameters for Anion-Anion Bonds in Solids", *Acta Cryst B*, **B48**, 152-154, (1991).
21. Ahrens, L. H., *Geochima and Cosmochima Acta*, **Vol. 2**, 155-164, (1952).
22. Shannon, R.D., *Acta Cryst.*, **A32**, 751-767, (1976)
23. Krüger H., Kahlenberg, V., "Incommensurately Modulated Ordering of Tetrahedral Chains in $\text{Ca}_2\text{Fe}_2\text{O}_5$ at Elevated Temperatures", *Acta Cryst. B*, **B61**, 656-662 (2005).
24. Berastegui, P., Eriksson, S.G., and Hull, S., "A Neutron Diffraction Study of the Temperature Dependence of $\text{Ca}_2\text{Fe}_2\text{O}_5$ ", *Materials Research Bulletin*, **Vol. 34**, No. 2, 303-314, (1999).
25. Heyes, S.J., "Structures of Simple Inorganic Solids", Oxford University, 1996-2000,
http://www.chem.ox.ac.uk/icl/heyes/structure_of_solids/Lecture2.
26. School of Physics at Georgia Tech, "Wave-Particle Duality", Georgia Tech University, September 1, 2002,
<http://www.physics.gatech.edu/advancedlab/labs/waveparticle/images/figure6.gif>.

27. Skakle, J., "Center for Diffraction Studies", University of Aberdeen, July, 2001, <http://www.abdn.ac.uk/~che241/cdiff/bragg.jpg>.
28. <http://content.answers.com/main/content/img/McGrawHill/Encyclopedia/images/CE675200FG0010.gif>
29. Foll, H., "Interpreting HRTEM Images", University of Kiel, http://www.tf.uni-kiel.de/matwis/amat/def_en/kap_2/illustr/perovskite.gif.
30. Lawrence Berkeley National Laboratory, "The Advanced Light Source", <http://www-als.lbl.gov>.

APPENDIX A**CRYSTALLOGRAPHIC DATA FOR SAMPLE AS $\text{Ca}_2\text{Mn}_2\text{N}_2\text{O}_2\text{F}$**

Table 1. Crystal data and structure refinement for $\text{Ca}_2\text{Mn}_2\text{N}_2\text{O}_2\text{F}$

Empirical formula	Ca ₂ Mn ₂ N ₂ O ₂ F
Formula weight	269.06
Temperature	273(2) K
Wavelength	0.77500 Å
Crystal system, space group	Orthorhombic, Imma (#74)
Unit cell dimensions	a = 14.736(4) Å alpha =
90°	b = 5.4397(16) Å beta =
90°	c = 5.6033(17) Å gamma =
90°	
Volume	449.1(2) Å ³
Z, Calculated density	4, 3.979 Mg/m ³
Absorption coefficient	7.815 mm ⁻¹
F(000)	516
Crystal size	? x ? x ? mm
Theta range for data collection	3.01 to 31.12 deg.
Limiting indices	-18<=h<=19, -7<=k<=6, -
7<=l<=7	
Reflections collected / unique	1721 / 324 [R(int) =
0.0364]	
Completeness to theta = 31.12	100.0 %
Refinement method	Full-matrix least-squares
on F ²	
Data / restraints / parameters	324 / 0 / 34
Goodness-of-fit on F ²	1.195
Final R indices [I>2sigma(I)]	R1 = 0.0382, wR2 = 0.0868
R indices (all data)	R1 = 0.0394, wR2 = 0.0874
Largest diff. peak and hole	0.930 and -0.759 e.Å ⁻³

Table 2. Atomic coordinates ($\times 10^4$) and equivalent isotropic displacement parameters ($\text{Å}^2 \times 10^3$) for $\text{Ca}_2\text{Mn}_2\text{N}_2\text{O}_2\text{F}$. $U(\text{eq})$ is defined as one third of the trace of the orthogonalized U_{ij} tensor.

		x	y	z
$U(\text{eq})$				
	Mn(1)	2500	2500	2500
7(1)	Mn(2)	5000	2945(3)	1849(3)
7(1)	Ca(1)	3584(1)	2500	7260(2)
13(1)	N(1)	3898(3)	2500	3205(9)
21(1)	O(1)	3898(3)	2500	3205(9)
21(1)	O(2)	2349(3)	0	5000
11(1)	N(3)	5000	3587(18)	-1231(16)
18(2)	F(3)	5000	3587(18)	-1231(16)
18(2)				

Table 3. Bond lengths [Å] and angles [deg] for $\text{Ca}_2\text{Mn}_2\text{N}_2\text{O}_2\text{F}$.

Mn(1)-O(2)#1	1.9649(6)
Mn(1)-O(2)	1.9649(6)
Mn(1)-O(2)#2	1.9649(6)
Mn(1)-O(2)#3	1.9649(6)
Mn(1)-O(1)#3	2.097(5)
Mn(1)-N(1)#3	2.097(5)
Mn(1)-N(1)	2.097(5)
Mn(1)-Ca(1)	3.1089(15)
Mn(1)-Ca(1)#3	3.1090(15)
Mn(1)-Ca(1)#1	3.1573(10)
Mn(1)-Ca(1)#4	3.1573(10)
Mn(2)-Mn(2)#5	0.484(4)
Mn(2)-N(3)	1.761(9)
Mn(2)-N(1)	1.809(5)
Mn(2)-O(1)#5	1.809(5)
Mn(2)-N(1)#5	1.809(5)
Mn(2)-F(3)#5	1.917(9)
Mn(2)-N(3)#5	1.917(9)
Mn(2)-F(3)#6	1.918(10)
Mn(2)-N(3)#6	1.918(10)
Mn(2)-F(3)#7	2.396(10)
Ca(1)-N(1)	2.318(5)
Ca(1)-F(3)#8	2.327(4)
Ca(1)-N(3)#8	2.327(4)
Ca(1)-F(3)#9	2.327(4)
Ca(1)-N(3)#9	2.327(4)
Ca(1)-O(2)#10	2.470(3)
Ca(1)-O(2)#11	2.470(3)
Ca(1)-O(2)	2.601(3)
Ca(1)-O(2)#1	2.601(3)
Ca(1)-O(1)#1	2.7711(13)
Ca(1)-N(1)#1	2.7711(13)
N(1)-Mn(2)#5	1.809(5)
N(1)-Ca(1)#4	2.7711(12)
N(1)-Ca(1)#1	2.7711(12)
O(2)-Mn(1)#11	1.9649(6)
O(2)-Ca(1)#10	2.470(3)
O(2)-Ca(1)#2	2.470(3)
O(2)-Ca(1)#4	2.601(3)
N(3)-F(3)#5	1.183(19)
N(3)-N(3)#5	1.183(19)
N(3)-Mn(2)#5	1.917(9)
N(3)-Mn(2)#6	1.918(10)
N(3)-Ca(1)#12	2.328(4)
N(3)-Ca(1)#13	2.328(4)
N(3)-Mn(2)#14	2.396(10)
O(2)#1-Mn(1)-O(2)	87.59(4)
O(2)#1-Mn(1)-O(2)#2	180.0
O(2)-Mn(1)-O(2)#2	92.41(4)
O(2)#1-Mn(1)-O(2)#3	92.41(4)
O(2)-Mn(1)-O(2)#3	180.0
O(2)#2-Mn(1)-O(2)#3	87.59(4)
O(2)#1-Mn(1)-O(1)#3	91.34(16)
O(2)-Mn(1)-O(1)#3	91.34(16)

O(2)#2-Mn(1)-O(1)#3	88.66(16)
O(2)#3-Mn(1)-O(1)#3	88.66(16)
O(2)#1-Mn(1)-N(1)#3	91.34(16)
O(2)-Mn(1)-N(1)#3	91.34(16)
O(2)#2-Mn(1)-N(1)#3	88.66(16)
O(2)#3-Mn(1)-N(1)#3	88.66(16)
O(1)#3-Mn(1)-N(1)#3	0.0(3)
O(2)#1-Mn(1)-N(1)	88.66(16)
O(2)-Mn(1)-N(1)	88.66(16)
O(2)#2-Mn(1)-N(1)	91.34(16)
O(2)#3-Mn(1)-N(1)	91.34(16)
O(1)#3-Mn(1)-N(1)	180.0
N(1)#3-Mn(1)-N(1)	180.0
O(2)#1-Mn(1)-Ca(1)	56.39(9)
O(2)-Mn(1)-Ca(1)	56.39(9)
O(2)#2-Mn(1)-Ca(1)	123.61(9)
O(2)#3-Mn(1)-Ca(1)	123.61(9)
O(1)#3-Mn(1)-Ca(1)	131.78(14)
N(1)#3-Mn(1)-Ca(1)	131.78(14)
N(1)-Mn(1)-Ca(1)	48.22(14)
O(2)#1-Mn(1)-Ca(1)#3	123.61(9)
O(2)-Mn(1)-Ca(1)#3	123.61(9)
O(2)#2-Mn(1)-Ca(1)#3	56.39(9)
O(2)#3-Mn(1)-Ca(1)#3	56.39(9)
O(1)#3-Mn(1)-Ca(1)#3	48.22(14)
N(1)#3-Mn(1)-Ca(1)#3	48.22(14)
N(1)-Mn(1)-Ca(1)#3	131.78(14)
Ca(1)-Mn(1)-Ca(1)#3	180.00(4)
O(2)#1-Mn(1)-Ca(1)#1	55.29(9)
O(2)-Mn(1)-Ca(1)#1	128.53(7)
O(2)#2-Mn(1)-Ca(1)#1	124.71(9)
O(2)#3-Mn(1)-Ca(1)#1	51.47(7)
O(1)#3-Mn(1)-Ca(1)#1	120.33(2)
N(1)#3-Mn(1)-Ca(1)#1	120.33(2)
N(1)-Mn(1)-Ca(1)#1	59.67(2)
Ca(1)-Mn(1)-Ca(1)#1	72.74(3)
Ca(1)#3-Mn(1)-Ca(1)#1	107.26(3)
O(2)#1-Mn(1)-Ca(1)#4	128.53(7)
O(2)-Mn(1)-Ca(1)#4	55.29(9)
O(2)#2-Mn(1)-Ca(1)#4	51.47(7)
O(2)#3-Mn(1)-Ca(1)#4	124.71(9)
O(1)#3-Mn(1)-Ca(1)#4	120.33(2)
N(1)#3-Mn(1)-Ca(1)#4	120.33(2)
N(1)-Mn(1)-Ca(1)#4	59.67(2)
Ca(1)-Mn(1)-Ca(1)#4	72.74(3)
Ca(1)#3-Mn(1)-Ca(1)#4	107.26(3)
Ca(1)#1-Mn(1)-Ca(1)#4	118.96(4)
Mn(2)#5-Mn(2)-N(3)	101.4(3)
Mn(2)#5-Mn(2)-N(1)	82.31(6)
N(3)-Mn(2)-N(1)	115.98(17)
Mn(2)#5-Mn(2)-O(1)#5	82.31(6)
N(3)-Mn(2)-O(1)#5	115.98(17)
N(1)-Mn(2)-O(1)#5	127.7(3)
Mn(2)#5-Mn(2)-N(1)#5	82.31(6)
N(3)-Mn(2)-N(1)#5	115.98(17)
N(1)-Mn(2)-N(1)#5	127.7(3)
O(1)#5-Mn(2)-N(1)#5	0.00(14)
Mn(2)#5-Mn(2)-F(3)#5	64.2(3)
N(3)-Mn(2)-F(3)#5	37.2(6)
N(1)-Mn(2)-F(3)#5	108.65(17)
O(1)#5-Mn(2)-F(3)#5	108.66(17)

N(1)#5-Mn(2)-F(3)#5	108.66(17)
Mn(2)#5-Mn(2)-N(3)#5	64.2(3)
N(3)-Mn(2)-N(3)#5	37.2(6)
N(1)-Mn(2)-N(3)#5	108.65(17)
O(1)#5-Mn(2)-N(3)#5	108.66(17)
N(1)#5-Mn(2)-N(3)#5	108.66(17)
F(3)#5-Mn(2)-N(3)#5	0.0(6)
Mn(2)#5-Mn(2)-F(3)#6	169.6(3)
N(3)-Mn(2)-F(3)#6	68.2(5)
N(1)-Mn(2)-F(3)#6	101.97(13)
O(1)#5-Mn(2)-F(3)#6	101.98(13)
N(1)#5-Mn(2)-F(3)#6	101.98(13)
F(3)#5-Mn(2)-F(3)#6	105.4(3)
N(3)#5-Mn(2)-F(3)#6	105.4(3)
Mn(2)#5-Mn(2)-N(3)#6	169.6(3)
N(3)-Mn(2)-N(3)#6	68.2(5)
N(1)-Mn(2)-N(3)#6	101.97(13)
O(1)#5-Mn(2)-N(3)#6	101.98(13)
N(1)#5-Mn(2)-N(3)#6	101.98(13)
F(3)#5-Mn(2)-N(3)#6	105.4(3)
N(3)#5-Mn(2)-N(3)#6	105.4(3)
F(3)#6-Mn(2)-N(3)#6	0.0(5)
Mn(2)#5-Mn(2)-F(3)#7	8.3(2)
N(3)-Mn(2)-F(3)#7	93.1(3)
N(1)-Mn(2)-F(3)#7	85.89(12)
O(1)#5-Mn(2)-F(3)#7	85.89(12)
N(1)#5-Mn(2)-F(3)#7	85.89(12)
F(3)#5-Mn(2)-F(3)#7	55.9(4)
N(3)#5-Mn(2)-F(3)#7	55.9(4)
F(3)#6-Mn(2)-F(3)#7	161.3(5)
N(3)#6-Mn(2)-F(3)#7	161.3(5)
N(1)-Ca(1)-F(3)#8	100.2(2)
N(1)-Ca(1)-N(3)#8	100.2(2)
F(3)#8-Ca(1)-N(3)#8	0.0(5)
N(1)-Ca(1)-F(3)#9	100.2(2)
F(3)#8-Ca(1)-F(3)#9	29.4(5)
N(3)#8-Ca(1)-F(3)#9	29.4(5)
N(1)-Ca(1)-N(3)#9	100.2(2)
F(3)#8-Ca(1)-N(3)#9	29.4(5)
N(3)#8-Ca(1)-N(3)#9	29.4(5)
F(3)#9-Ca(1)-N(3)#9	0.0(5)
N(1)-Ca(1)-O(2)#10	136.07(9)
F(3)#8-Ca(1)-O(2)#10	97.7(2)
N(3)#8-Ca(1)-O(2)#10	97.7(2)
F(3)#9-Ca(1)-O(2)#10	114.4(2)
N(3)#9-Ca(1)-O(2)#10	114.4(2)
N(1)-Ca(1)-O(2)#11	136.07(9)
F(3)#8-Ca(1)-O(2)#11	114.4(2)
N(3)#8-Ca(1)-O(2)#11	114.4(2)
F(3)#9-Ca(1)-O(2)#11	97.7(2)
N(3)#9-Ca(1)-O(2)#11	97.7(2)
O(2)#10-Ca(1)-O(2)#11	66.82(8)
N(1)-Ca(1)-O(2)	70.27(12)
F(3)#8-Ca(1)-O(2)	159.5(2)
N(3)#8-Ca(1)-O(2)	159.5(2)
F(3)#9-Ca(1)-O(2)	132.2(2)
N(3)#9-Ca(1)-O(2)	132.2(2)
O(2)#10-Ca(1)-O(2)	101.58(5)
O(2)#11-Ca(1)-O(2)	67.97(4)
N(1)-Ca(1)-O(2)#1	70.27(12)
F(3)#8-Ca(1)-O(2)#1	132.2(2)

N(3)#8-Ca(1)-O(2)#1	132.2(2)
F(3)#9-Ca(1)-O(2)#1	159.5(2)
N(3)#9-Ca(1)-O(2)#1	159.5(2)
O(2)#10-Ca(1)-O(2)#1	67.98(4)
O(2)#11-Ca(1)-O(2)#1	101.58(5)
O(2)-Ca(1)-O(2)#1	63.05(9)
N(1)-Ca(1)-O(1)#1	82.80(12)
F(3)#8-Ca(1)-O(1)#1	68.6(3)
N(3)#8-Ca(1)-O(1)#1	68.6(3)
F(3)#9-Ca(1)-O(1)#1	97.7(3)
N(3)#9-Ca(1)-O(1)#1	97.7(3)
O(2)#10-Ca(1)-O(1)#1	67.10(11)
O(2)#11-Ca(1)-O(1)#1	133.77(11)
O(2)-Ca(1)-O(1)#1	125.74(12)
O(2)#1-Ca(1)-O(1)#1	63.75(12)
N(1)-Ca(1)-N(1)#1	82.80(12)
F(3)#8-Ca(1)-N(1)#1	68.6(3)
N(3)#8-Ca(1)-N(1)#1	68.6(3)
F(3)#9-Ca(1)-N(1)#1	97.7(3)
N(3)#9-Ca(1)-N(1)#1	97.7(3)
O(2)#10-Ca(1)-N(1)#1	67.10(11)
O(2)#11-Ca(1)-N(1)#1	133.77(11)
O(2)-Ca(1)-N(1)#1	125.74(12)
O(2)#1-Ca(1)-N(1)#1	63.75(12)
O(1)#1-Ca(1)-N(1)#1	0.0(2)
Mn(2)#5-N(1)-Mn(2)	15.38(12)
Mn(2)#5-N(1)-Mn(1)	143.4(3)
Mn(2)-N(1)-Mn(1)	143.4(3)
Mn(2)#5-N(1)-Ca(1)	126.2(3)
Mn(2)-N(1)-Ca(1)	126.2(3)
Mn(1)-N(1)-Ca(1)	89.36(19)
Mn(2)#5-N(1)-Ca(1)#4	88.79(11)
Mn(2)-N(1)-Ca(1)#4	103.98(14)
Mn(1)-N(1)-Ca(1)#4	79.55(10)
Ca(1)-N(1)-Ca(1)#4	93.37(11)
Mn(2)#5-N(1)-Ca(1)#1	103.98(14)
Mn(2)-N(1)-Ca(1)#1	88.79(11)
Mn(1)-N(1)-Ca(1)#1	79.55(10)
Ca(1)-N(1)-Ca(1)#1	93.37(11)
Ca(1)#4-N(1)-Ca(1)#1	157.9(2)
Mn(1)#11-O(2)-Mn(1)	167.0(2)
Mn(1)#11-O(2)-Ca(1)#10	90.05(6)
Mn(1)-O(2)-Ca(1)#10	97.19(7)
Mn(1)#11-O(2)-Ca(1)#2	97.19(7)
Mn(1)-O(2)-Ca(1)#2	90.05(6)
Ca(1)#10-O(2)-Ca(1)#2	112.30(17)
Mn(1)#11-O(2)-Ca(1)#4	84.61(9)
Mn(1)-O(2)-Ca(1)#4	86.32(9)
Ca(1)#10-O(2)-Ca(1)#4	168.62(14)
Ca(1)#2-O(2)-Ca(1)#4	78.41(5)
Mn(1)#11-O(2)-Ca(1)	86.32(9)
Mn(1)-O(2)-Ca(1)	84.61(9)
Ca(1)#10-O(2)-Ca(1)	78.41(5)
Ca(1)#2-O(2)-Ca(1)	168.62(14)
Ca(1)#4-O(2)-Ca(1)	91.19(14)
F(3)#5-N(3)-N(3)#5	0.0(9)
F(3)#5-N(3)-Mn(2)	78.6(3)
N(3)#5-N(3)-Mn(2)	78.6(3)
F(3)#5-N(3)-Mn(2)#5	64.2(3)
N(3)#5-N(3)-Mn(2)#5	64.2(3)
Mn(2)-N(3)-Mn(2)#5	14.34(13)

F(3)#5-N(3)-Mn(2)#6	169.6(3)
N(3)#5-N(3)-Mn(2)#6	169.6(3)
Mn(2)-N(3)-Mn(2)#6	111.9(5)
Mn(2)#5-N(3)-Mn(2)#6	126.2(5)
F(3)#5-N(3)-Ca(1)#12	75.3(2)
N(3)#5-N(3)-Ca(1)#12	75.3(2)
Mn(2)-N(3)-Ca(1)#12	107.8(3)
Mn(2)#5-N(3)-Ca(1)#12	102.5(3)
Mn(2)#6-N(3)-Ca(1)#12	100.6(3)
F(3)#5-N(3)-Ca(1)#13	75.3(2)
N(3)#5-N(3)-Ca(1)#13	75.3(2)
Mn(2)-N(3)-Ca(1)#13	107.8(3)
Mn(2)#5-N(3)-Ca(1)#13	102.5(3)
Mn(2)#6-N(3)-Ca(1)#13	100.6(3)
Ca(1)#12-N(3)-Ca(1)#13	127.4(4)
F(3)#5-N(3)-Mn(2)#14	171.7(2)
N(3)#5-N(3)-Mn(2)#14	171.7(2)
Mn(2)-N(3)-Mn(2)#14	109.8(4)
Mn(2)#5-N(3)-Mn(2)#14	124.1(4)
Mn(2)#6-N(3)-Mn(2)#14	2.09(6)
Ca(1)#12-N(3)-Mn(2)#14	101.5(3)
Ca(1)#13-N(3)-Mn(2)#14	101.5(3)

atoms: Symmetry transformations used to generate equivalent

#1 $x, y+1/2, -z+1$ #2 $-x+1/2, -y+0, z-1/2$
 #3 $-x+1/2, -y+1/2, -z+1/2$ #4 $x, y-1/2, -z+1$
 #5 $-x+1, -y+1/2, z$ #6 $-x+1, -y+1, -z$
 #7 $x, y-1/2, -z$ #8 $x, y, z+1$ #9 $-x+1, -y+1/2, z+1$
 #10 $-x+1/2, -y+1/2, -z+3/2$ #11 $-x+1/2, -y+0, z+1/2$
 #12 $-x+1, -y+1/2, z-1$ #13 $x, y, z-1$ #14 $x, y+1/2, -z$

Table 4. Anisotropic displacement parameters ($\text{\AA}^2 \times 10^3$) for $\text{Ca}_2\text{Mn}_2\text{N}_2\text{O}_2\text{F}$.

The anisotropic displacement factor exponent takes the form:
 $-2 \pi^2 [h^2 a^{*2} U_{11} + \dots + 2 h k a^* b^* U_{12}]$

U12		U11	U22	U33	U23	U13
0	Mn(1)	7(1)	6(1)	7(1)	0	0(1)
0	Mn(2)	3(1)	6(2)	14(1)	1(1)	0
0	Ca(1)	7(1)	18(1)	13(1)	0	0(1)
0	N(1)	6(2)	46(4)	9(2)	0	-1(2)
0	O(1)	6(2)	46(4)	9(2)	0	-1(2)
0	O(2)	16(2)	7(2)	12(2)	2(2)	0
0	N(3)	16(4)	17(4)	20(4)	1(4)	0
0	F(3)	16(4)	17(4)	20(4)	1(4)	0

APPENDIX B**CRYSTALLOGRAPHIC DATA FOR $\text{Ca}_2\text{Fe}_2\text{O}_5$**

Table 1. Crystal data and structure refinement for $\text{Ca}_2\text{Fe}_2\text{O}_5$.

Empirical formula	Ca ₂ F Fe ₂ N O ₃
Formula weight	272.87
Temperature	273(2) K
Wavelength	0.77500 Å
Crystal system, space group	orthorhombic, Imma (#74)
Unit cell dimensions	a = 14.736(4) Å alpha =
90°	b = 5.4397(16) Å beta =
90°	c = 5.6033(17) Å gamma =
90°	
Volume	449.1(2) Å ³
Z, Calculated density	4, 4.035 Mg/m ³
Absorption coefficient	8.664 mm ⁻¹
F(000)	528
Crystal size	? x ? x ? mm
Theta range for data collection	3.01 to 31.12 deg.
Limiting indices	-18<=h<=19, -7<=k<=6, -
7<=l<=7	
Reflections collected / unique	1721 / 324 [R(int) =
0.0364]	
Completeness to theta = 31.12	100.0 %
Refinement method	Full-matrix least-squares
on F ²	
Data / restraints / parameters	324 / 0 / 36
Goodness-of-fit on F ²	1.062
Final R indices [I>2sigma(I)]	R1 = 0.0351, wR2 = 0.0901
R indices (all data)	R1 = 0.0364, wR2 = 0.0908
Largest diff. peak and hole	0.880 and -0.773 e.Å ⁻³

Table 2. Atomic coordinates ($\times 10^4$) and equivalent isotropic displacement parameters ($\text{Å}^2 \times 10^3$) for $\text{Ca}_2\text{Fe}_2\text{O}_5$. $U(\text{eq})$ is defined as one third of the trace of the orthogonalized U_{ij} tensor.

		x	y	z
U(eq)				
11(1)	Ca(1)	3584(1)	2500	7260(2)
	Fe(1)	2500	2500	2500
7(1)	Fe(2)	5000	2945(3)	1848(3)
9(1)	O(1)	3892(3)	2500	3204(9)
25(1)	O(2)	2350(3)	0	5000
9(1)	O(3)	5000	3574(17)	-1234(15)
12(2)				

Table 3. Bond lengths [Å] and angles [deg] for $\text{Ca}_2\text{Fe}_2\text{O}_5$.

Ca(1)-O(1)	2.318(5)
Ca(1)-O(3)#1	2.326(4)
Ca(1)-O(3)#2	2.326(4)
Ca(1)-O(2)#3	2.470(2)
Ca(1)-O(2)#4	2.470(2)
Ca(1)-O(2)#5	2.600(3)
Ca(1)-O(2)	2.600(3)
Ca(1)-O(1)#5	2.7698(12)
Ca(1)-O(1)#6	2.7698(12)
Ca(1)-Fe(1)	3.1087(14)
Ca(1)-Fe(1)#4	3.1570(10)
Ca(1)-Fe(1)#7	3.1570(10)
Fe(1)-O(2)#8	1.9648(6)
Fe(1)-O(2)#9	1.9648(6)
Fe(1)-O(2)	1.9649(6)
Fe(1)-O(2)#5	1.9649(6)
Fe(1)-O(1)#9	2.089(5)
Fe(1)-O(1)	2.089(5)
Fe(1)-Ca(1)#9	3.1087(14)
Fe(1)-Ca(1)#8	3.1570(10)
Fe(1)-Ca(1)#10	3.1570(9)
Fe(1)-Ca(1)#5	3.1570(10)
Fe(1)-Ca(1)#6	3.1570(10)
Fe(2)-Fe(2)#11	0.484(4)
Fe(2)-O(3)	1.761(9)
Fe(2)-O(1)	1.817(5)
Fe(2)-O(1)#11	1.817(5)
Fe(2)-O(3)#11	1.915(9)
Fe(2)-O(3)#12	1.925(10)
Fe(2)-Ca(1)#5	3.2778(18)
Fe(2)-Ca(1)#13	3.2779(18)
Fe(2)-Ca(1)#14	3.3201(19)
Fe(2)-Ca(1)#15	3.3201(19)
Fe(2)-Ca(1)#6	3.6574(18)
Fe(2)-Ca(1)#16	3.6575(18)
O(1)-Fe(2)#11	1.817(5)
O(1)-Ca(1)#6	2.7697(12)
O(1)-Ca(1)#5	2.7697(12)
O(2)-Fe(1)#4	1.9649(6)
O(2)-Ca(1)#8	2.470(2)
O(2)-Ca(1)#3	2.470(2)
O(2)-Ca(1)#6	2.600(3)
O(3)-O(3)#11	1.168(19)
O(3)-Fe(2)#11	1.915(9)
O(3)-Fe(2)#12	1.925(10)
O(3)-Ca(1)#14	2.325(4)
O(3)-Ca(1)#15	2.326(4)
O(1)-Ca(1)-O(3)#1	100.4(2)
O(1)-Ca(1)-O(3)#2	100.4(2)
O(3)#1-Ca(1)-O(3)#2	29.1(5)
O(1)-Ca(1)-O(2)#3	135.96(9)
O(3)#1-Ca(1)-O(2)#3	97.8(2)
O(3)#2-Ca(1)-O(2)#3	114.4(2)
O(1)-Ca(1)-O(2)#4	135.96(9)

O(3)#1-Ca(1)-O(2)#4	114.4(2)
O(3)#2-Ca(1)-O(2)#4	97.8(2)
O(2)#3-Ca(1)-O(2)#4	66.82(8)
O(1)-Ca(1)-O(2)#5	70.10(11)
O(3)#1-Ca(1)-O(2)#5	132.3(2)
O(3)#2-Ca(1)-O(2)#5	159.3(2)
O(2)#3-Ca(1)-O(2)#5	67.98(4)
O(2)#4-Ca(1)-O(2)#5	101.61(5)
O(1)-Ca(1)-O(2)	70.10(11)
O(3)#1-Ca(1)-O(2)	159.3(2)
O(3)#2-Ca(1)-O(2)	132.3(2)
O(2)#3-Ca(1)-O(2)	101.61(5)
O(2)#4-Ca(1)-O(2)	67.98(4)
O(2)#5-Ca(1)-O(2)	63.08(8)
O(1)-Ca(1)-O(1)#5	82.87(11)
O(3)#1-Ca(1)-O(1)#5	68.9(3)
O(3)#2-Ca(1)-O(1)#5	97.7(2)
O(2)#3-Ca(1)-O(1)#5	66.98(11)
O(2)#4-Ca(1)-O(1)#5	133.66(11)
O(2)#5-Ca(1)-O(1)#5	63.61(11)
O(2)-Ca(1)-O(1)#5	125.64(11)
O(1)-Ca(1)-O(1)#6	82.87(11)
O(3)#1-Ca(1)-O(1)#6	97.7(2)
O(3)#2-Ca(1)-O(1)#6	68.9(3)
O(2)#3-Ca(1)-O(1)#6	133.66(11)
O(2)#4-Ca(1)-O(1)#6	66.98(11)
O(2)#5-Ca(1)-O(1)#6	125.64(11)
O(2)-Ca(1)-O(1)#6	63.61(11)
O(1)#5-Ca(1)-O(1)#6	158.2(2)
O(1)-Ca(1)-Fe(1)	42.22(12)
O(3)#1-Ca(1)-Fe(1)	140.6(2)
O(3)#2-Ca(1)-Fe(1)	140.6(2)
O(2)#3-Ca(1)-Fe(1)	104.31(7)
O(2)#4-Ca(1)-Fe(1)	104.31(7)
O(2)#5-Ca(1)-Fe(1)	38.997(19)
O(2)-Ca(1)-Fe(1)	38.997(19)
O(1)#5-Ca(1)-Fe(1)	90.22(10)
O(1)#6-Ca(1)-Fe(1)	90.22(11)
O(1)-Ca(1)-Fe(1)#4	98.11(6)
O(3)#1-Ca(1)-Fe(1)#4	130.9(2)
O(3)#2-Ca(1)-Fe(1)#4	102.8(2)
O(2)#3-Ca(1)-Fe(1)#4	99.56(7)
O(2)#4-Ca(1)-Fe(1)#4	38.491(16)
O(2)#5-Ca(1)-Fe(1)#4	96.75(7)
O(2)-Ca(1)-Fe(1)#4	38.398(13)
O(1)#5-Ca(1)-Fe(1)#4	158.91(11)
O(1)#6-Ca(1)-Fe(1)#4	40.62(10)
Fe(1)-Ca(1)-Fe(1)#4	77.10(2)
O(1)-Ca(1)-Fe(1)#7	98.11(6)
O(3)#1-Ca(1)-Fe(1)#7	102.8(2)
O(3)#2-Ca(1)-Fe(1)#7	130.9(2)
O(2)#3-Ca(1)-Fe(1)#7	38.491(16)
O(2)#4-Ca(1)-Fe(1)#7	99.56(7)
O(2)#5-Ca(1)-Fe(1)#7	38.398(13)
O(2)-Ca(1)-Fe(1)#7	96.75(7)
O(1)#5-Ca(1)-Fe(1)#7	40.62(10)
O(1)#6-Ca(1)-Fe(1)#7	158.91(11)
Fe(1)-Ca(1)-Fe(1)#7	77.10(2)
Fe(1)#4-Ca(1)-Fe(1)#7	118.98(4)
O(2)#8-Fe(1)-O(2)#9	87.60(3)
O(2)#8-Fe(1)-O(2)	92.40(3)

O(2)#9-Fe(1)-O(2)	180.0
O(2)#8-Fe(1)-O(2)#5	180.0
O(2)#9-Fe(1)-O(2)#5	92.40(3)
O(2)-Fe(1)-O(2)#5	87.60(3)
O(2)#8-Fe(1)-O(1)#9	88.63(15)
O(2)#9-Fe(1)-O(1)#9	88.63(15)
O(2)-Fe(1)-O(1)#9	91.37(15)
O(2)#5-Fe(1)-O(1)#9	91.37(15)
O(2)#8-Fe(1)-O(1)	91.37(15)
O(2)#9-Fe(1)-O(1)	91.37(15)
O(2)-Fe(1)-O(1)	88.63(15)
O(2)#5-Fe(1)-O(1)	88.63(15)
O(1)#9-Fe(1)-O(1)	180.0
O(2)#8-Fe(1)-Ca(1)#9	56.37(8)
O(2)#9-Fe(1)-Ca(1)#9	56.37(8)
O(2)-Fe(1)-Ca(1)#9	123.63(8)
O(2)#5-Fe(1)-Ca(1)#9	123.63(8)
O(1)#9-Fe(1)-Ca(1)#9	48.21(14)
O(1)-Fe(1)-Ca(1)#9	131.79(14)
O(2)#8-Fe(1)-Ca(1)	123.63(8)
O(2)#9-Fe(1)-Ca(1)	123.63(8)
O(2)-Fe(1)-Ca(1)	56.37(8)
O(2)#5-Fe(1)-Ca(1)	56.37(8)
O(1)#9-Fe(1)-Ca(1)	131.79(14)
O(1)-Fe(1)-Ca(1)	48.21(14)
Ca(1)#9-Fe(1)-Ca(1)	180.0
O(2)#8-Fe(1)-Ca(1)#8	55.27(8)
O(2)#9-Fe(1)-Ca(1)#8	128.53(7)
O(2)-Fe(1)-Ca(1)#8	51.47(7)
O(2)#5-Fe(1)-Ca(1)#8	124.73(8)
O(1)#9-Fe(1)-Ca(1)#8	59.68(2)
O(1)-Fe(1)-Ca(1)#8	120.32(2)
Ca(1)#9-Fe(1)-Ca(1)#8	72.75(3)
Ca(1)-Fe(1)-Ca(1)#8	107.25(3)
O(2)#8-Fe(1)-Ca(1)#10	128.53(7)
O(2)#9-Fe(1)-Ca(1)#10	55.27(8)
O(2)-Fe(1)-Ca(1)#10	124.73(8)
O(2)#5-Fe(1)-Ca(1)#10	51.47(7)
O(1)#9-Fe(1)-Ca(1)#10	59.68(2)
O(1)-Fe(1)-Ca(1)#10	120.32(2)
Ca(1)#9-Fe(1)-Ca(1)#10	72.75(3)
Ca(1)-Fe(1)-Ca(1)#10	107.25(3)
Ca(1)#8-Fe(1)-Ca(1)#10	118.98(4)
O(2)#8-Fe(1)-Ca(1)#5	124.73(8)
O(2)#9-Fe(1)-Ca(1)#5	51.47(7)
O(2)-Fe(1)-Ca(1)#5	128.53(7)
O(2)#5-Fe(1)-Ca(1)#5	55.27(8)
O(1)#9-Fe(1)-Ca(1)#5	120.32(2)
O(1)-Fe(1)-Ca(1)#5	59.68(2)
Ca(1)#9-Fe(1)-Ca(1)#5	107.25(3)
Ca(1)-Fe(1)-Ca(1)#5	72.75(3)
Ca(1)#8-Fe(1)-Ca(1)#5	180.0
Ca(1)#10-Fe(1)-Ca(1)#5	61.02(4)
O(2)#8-Fe(1)-Ca(1)#6	51.47(7)
O(2)#9-Fe(1)-Ca(1)#6	124.73(8)
O(2)-Fe(1)-Ca(1)#6	55.27(8)
O(2)#5-Fe(1)-Ca(1)#6	128.53(7)
O(1)#9-Fe(1)-Ca(1)#6	120.32(2)
O(1)-Fe(1)-Ca(1)#6	59.68(2)
Ca(1)#9-Fe(1)-Ca(1)#6	107.25(3)
Ca(1)-Fe(1)-Ca(1)#6	72.75(3)

Ca(1)#8-Fe(1)-Ca(1)#6	61.02(4)
Ca(1)#10-Fe(1)-Ca(1)#6	180.0
Ca(1)#5-Fe(1)-Ca(1)#6	118.98(4)
Fe(2)#11-Fe(2)-O(3)	101.2(3)
Fe(2)#11-Fe(2)-O(1)	82.35(6)
O(3)-Fe(2)-O(1)	115.85(16)
Fe(2)#11-Fe(2)-O(1)#11	82.34(6)
O(3)-Fe(2)-O(1)#11	115.85(16)
O(1)-Fe(2)-O(1)#11	127.9(3)
Fe(2)#11-Fe(2)-O(3)#11	64.4(3)
O(3)-Fe(2)-O(3)#11	36.8(6)
O(1)-Fe(2)-O(3)#11	108.65(17)
O(1)#11-Fe(2)-O(3)#11	108.64(17)
Fe(2)#11-Fe(2)-O(3)#12	169.7(3)
O(3)-Fe(2)-O(3)#12	68.5(5)
O(1)-Fe(2)-O(3)#12	101.87(12)
O(1)#11-Fe(2)-O(3)#12	101.87(12)
O(3)#11-Fe(2)-O(3)#12	105.3(3)
Fe(2)#11-Fe(2)-Ca(1)#5	139.11(3)
O(3)-Fe(2)-Ca(1)#5	90.2(2)
O(1)-Fe(2)-Ca(1)#5	57.65(5)
O(1)#11-Fe(2)-Ca(1)#5	127.52(11)
O(3)#11-Fe(2)-Ca(1)#5	117.6(2)
O(3)#12-Fe(2)-Ca(1)#5	44.23(11)
Fe(2)#11-Fe(2)-Ca(1)#13	139.10(3)
O(3)-Fe(2)-Ca(1)#13	90.2(2)
O(1)-Fe(2)-Ca(1)#13	127.52(11)
O(1)#11-Fe(2)-Ca(1)#13	57.65(5)
O(3)#11-Fe(2)-Ca(1)#13	117.6(2)
O(3)#12-Fe(2)-Ca(1)#13	44.23(11)
Ca(1)#5-Fe(2)-Ca(1)#13	79.08(6)
Fe(2)#11-Fe(2)-Ca(1)#14	85.82(3)
O(3)-Fe(2)-Ca(1)#14	41.80(11)
O(1)-Fe(2)-Ca(1)#14	75.48(16)
O(1)#11-Fe(2)-Ca(1)#14	151.50(16)
O(3)#11-Fe(2)-Ca(1)#14	43.11(11)
O(3)#12-Fe(2)-Ca(1)#14	86.2(2)
Ca(1)#5-Fe(2)-Ca(1)#14	76.88(4)
Ca(1)#13-Fe(2)-Ca(1)#14	124.98(6)
Fe(2)#11-Fe(2)-Ca(1)#15	85.82(3)
O(3)-Fe(2)-Ca(1)#15	41.80(11)
O(1)-Fe(2)-Ca(1)#15	151.50(16)
O(1)#11-Fe(2)-Ca(1)#15	75.48(16)
O(3)#11-Fe(2)-Ca(1)#15	43.11(11)
O(3)#12-Fe(2)-Ca(1)#15	86.2(2)
Ca(1)#5-Fe(2)-Ca(1)#15	124.98(6)
Ca(1)#13-Fe(2)-Ca(1)#15	76.88(4)
Ca(1)#14-Fe(2)-Ca(1)#15	77.88(6)
Fe(2)#11-Fe(2)-Ca(1)#6	35.93(3)
O(3)-Fe(2)-Ca(1)#6	106.9(3)
O(1)-Fe(2)-Ca(1)#6	47.34(6)
O(1)#11-Fe(2)-Ca(1)#6	110.35(10)
O(3)#11-Fe(2)-Ca(1)#6	76.9(2)
O(3)#12-Fe(2)-Ca(1)#6	145.21(3)
Ca(1)#5-Fe(2)-Ca(1)#6	103.19(4)
Ca(1)#13-Fe(2)-Ca(1)#6	162.66(7)
Ca(1)#14-Fe(2)-Ca(1)#6	71.83(4)
Ca(1)#15-Fe(2)-Ca(1)#6	113.92(5)
Fe(2)#11-Fe(2)-Ca(1)#16	35.92(3)
O(3)-Fe(2)-Ca(1)#16	106.9(3)
O(1)-Fe(2)-Ca(1)#16	110.35(10)

O(1)#11-Fe(2)-Ca(1)#16	47.34(5)
O(3)#11-Fe(2)-Ca(1)#16	76.9(2)
O(3)#12-Fe(2)-Ca(1)#16	145.20(3)
Ca(1)#5-Fe(2)-Ca(1)#16	162.66(7)
Ca(1)#13-Fe(2)-Ca(1)#16	103.18(4)
Ca(1)#14-Fe(2)-Ca(1)#16	113.92(5)
Ca(1)#15-Fe(2)-Ca(1)#16	71.83(4)
Ca(1)#6-Fe(2)-Ca(1)#16	69.58(5)
Fe(2)-O(1)-Fe(2)#11	15.31(12)
Fe(2)-O(1)-Fe(1)	143.5(3)
Fe(2)#11-O(1)-Fe(1)	143.5(3)
Fe(2)-O(1)-Ca(1)	125.9(2)
Fe(2)#11-O(1)-Ca(1)	125.9(2)
Fe(1)-O(1)-Ca(1)	89.57(18)
Fe(2)-O(1)-Ca(1)#6	103.83(14)
Fe(2)#11-O(1)-Ca(1)#6	88.71(10)
Fe(1)-O(1)-Ca(1)#6	79.70(10)
Ca(1)-O(1)-Ca(1)#6	93.43(11)
Fe(2)-O(1)-Ca(1)#5	88.71(10)
Fe(2)#11-O(1)-Ca(1)#5	103.83(14)
Fe(1)-O(1)-Ca(1)#5	79.70(10)
Ca(1)-O(1)-Ca(1)#5	93.43(11)
Ca(1)#6-O(1)-Ca(1)#5	158.2(2)
Fe(1)-O(2)-Fe(1)#4	167.1(2)
Fe(1)-O(2)-Ca(1)#8	90.04(6)
Fe(1)#4-O(2)-Ca(1)#8	97.17(7)
Fe(1)-O(2)-Ca(1)#3	97.17(7)
Fe(1)#4-O(2)-Ca(1)#3	90.04(6)
Ca(1)#8-O(2)-Ca(1)#3	112.30(16)
Fe(1)-O(2)-Ca(1)	84.63(9)
Fe(1)#4-O(2)-Ca(1)	86.33(9)
Ca(1)#8-O(2)-Ca(1)	168.64(13)
Ca(1)#3-O(2)-Ca(1)	78.39(5)
Fe(1)-O(2)-Ca(1)#6	86.33(9)
Fe(1)#4-O(2)-Ca(1)#6	84.63(9)
Ca(1)#8-O(2)-Ca(1)#6	78.39(5)
Ca(1)#3-O(2)-Ca(1)#6	168.64(13)
Ca(1)-O(2)-Ca(1)#6	91.24(14)
O(3)#11-O(3)-Fe(2)	78.8(3)
O(3)#11-O(3)-Fe(2)#11	64.4(3)
Fe(2)-O(3)-Fe(2)#11	14.36(13)
O(3)#11-O(3)-Fe(2)#12	169.7(3)
Fe(2)-O(3)-Fe(2)#12	111.5(5)
Fe(2)#11-O(3)-Fe(2)#12	125.9(5)
O(3)#11-O(3)-Ca(1)#14	75.5(2)
Fe(2)-O(3)-Ca(1)#14	107.9(2)
Fe(2)#11-O(3)-Ca(1)#14	102.6(3)
Fe(2)#12-O(3)-Ca(1)#14	100.5(3)
O(3)#11-O(3)-Ca(1)#15	75.4(2)
Fe(2)-O(3)-Ca(1)#15	107.9(2)
Fe(2)#11-O(3)-Ca(1)#15	102.6(3)
Fe(2)#12-O(3)-Ca(1)#15	100.5(3)
Ca(1)#14-O(3)-Ca(1)#15	127.6(4)

Symmetry transformations used to generate equivalent

atoms:

#1 $x, y, z+1$ #2 $-x+1, -y+1/2, z+1$ #3 $-x+1/2, -y+1/2, z+3/2$
#4 $-x+1/2, -y+0, z+1/2$ #5 $x, y+1/2, -z+1$

#6 $x, y-1/2, -z+1$ #7 $-x+1/2, -y+1, z+1/2$
#8 $-x+1/2, -y+0, z-1/2$ #9 $-x+1/2, -y+1/2, -z+1/2$
#10 $-x+1/2, -y+1, z-1/2$ #11 $-x+1, -y+1/2, z$
#12 $-x+1, -y+1, -z$ #13 $-x+1, -y+1, -z+1$
#14 $x, y, z-1$ #15 $-x+1, -y+1/2, z-1$ #16 $-x+1, -y, -z+1$

Table 4. Anisotropic displacement parameters ($\text{\AA}^2 \times 10^3$) for $\text{Ca}_2\text{Fe}_2\text{O}_5$.

The anisotropic displacement factor exponent takes the form:
 $-2 \pi^2 [h^2 a^{*2} U_{11} + \dots + 2 h k a^* b^* U_{12}]$

	U11	U22	U33	U23	U13	
U12						
0	Ca(1)	6(1)	16(1)	11(1)	0	0(1)
0	Fe(1)	9(1)	6(1)	7(1)	0	0(1)
0	Fe(2)	3(1)	8(2)	15(1)	1(1)	0
0	O(1)	9(2)	52(4)	12(2)	0	0(2)
0	O(2)	13(2)	4(2)	10(2)	1(2)	0
0	O(3)	11(4)	12(4)	12(4)	2(4)	0